TAMPEREEN TEKNILLINEN YLIOPISTO
TAMPERE UNIVERSITY OF TECHNOLOGY

VILIJUS BURZDŽIUS

Effect of Orthognathic Surgery on the Upper Airway System

Master's thesis

Examiners: Prof. Hannu Eskola, Adj. Prof. Prasun Dastidar.
Examiners and topic approved by the Faculty Council of the Faculty of Natural Sciences on 8 November 2013.

ABSTRACT
TAMPERE UNIVERSITY OF TECHNOLOGY
International Master's Degree Programme in Biomedical Engineering
BURZDŽIUS, VILIJUS: Effect of Orthognathic Surgery on the Upper Airway System
Master of Science Thesis, 54 pages, 1 Appendix page
February 2014
Major subject: Medical physics
Examiners: Professor Hannu Eskola, Adj. Professor Prasun Dastidar
Keywords: sleep apnea, MRI segmentation, orthognathic surgery, airflow modelling, upper airways

Sleep apnea is a disease which has not been getting an adequate amount of attention in the research community for a long time. However, the strain on the cardiovascular system and other serious problems, such as daytime sleepiness and even neurocognitive dysfunction, that it causes may be severe in advanced cases of the illness, as such it can significantly affect the heart especially and lead to cardiac arrest. Thus, it has been receiving a lot of attention recently. Tampere University Hospital has a goal of creating a comprehensive upper airway airflow model for surgery outcome prediction. That requires knowledge of available models and analysis of static magnetic resonance images, among other things. This document deals with these two main issues.

This thesis has two major parts, one of them being a literature review of sleep apnea and models used in airflow modelling in the upper airways. Modelling of airflow generally includes acquisition of a static upper airway system model (in the case of upper airway modelling) and then adding a dynamic component to it. The second part of this thesis deals with acquisition of the static model, which involves segmentation of MRI image sets from 3 patients (pre- and post-operative sequences). It also answers the question, whether the effect of orhtognathic surgery on the upper airway system can be seen from volumetric analysis of the segmented images and the segmented images themselves.

The main methods of adding a dynamic component to the static model turned out to be computational fluid mechanics and finite element modelling, including their sub-methods, such as direct numerical simulation of large eddy simulation. As with the second part of the thesis, the volumetric segmentation data is rather inconclusive and should not be related solely for evaluation of the effect of orthognathic surgery on the upper airway system. It can be said, nonetheless, that the volume of the upper airway itself is rather easily obtainable and reliable. The images themselves, however, provide very visual information about that, and shifting of certain muscles and muscle groups and other structures can be seen.

PREFACE

This thesis is an original intellectual product of Vilijus Burzdžius. I would like to thank my supervisors prof. Hannu Eskola and adj. prof. Prasun Dastidar, DDS Jorma Järnstedt for advice and help during the work,. In addition, special thanks to my fellow student Antti Paldanius, who got me acquainted with the segmentation software used in this thesis.

Tampere, February 2014 Vilijus Burzdžius

Table of Contents

List of terms, symbols and abbreviations

Catecholamine surge - build up of certain compounds in the body, with effects similar to an adrenaline rush
CBCT - Cone beam computed tomography
CFD - Computational fluid dynamics
CSA - Central sleep apnea
CT - Computed tomography
DNS - Direct numerical simulation
DICOM - In the case of this work, the format of used magnetic resonance images. The abbreviation stands for Digital Imaging and Communications in Medicine
FEM - Finite element modelling
Genioglossus - tongue muscle
LES - Large eddy simulation
MRI - Magnetic resonance imaging
OSA - Obstructive sleep apnea

Introduction

Sleep apnea is a sleep associated breathing disorder than has been receiving a lot of attention recently. This is mainly due to the fact that it is quite widespread and may cause rather severe problems, mainly associated with the cardiovascular system. (Eckert et al. 2009.) There are many treatment options available, starting from external breathing assisting devices, such as the continuous pharyngeal pressure device, certain medication, up to various surgical intervention methods. (Simon & Zieve 2012.) This thesis mainly deals with the surgical treatment, in a way that the data (magnetic resonance imaging data in this case) was acquired from orthognathic surgery patients and the static model acquisition (described in later chapters of this thesis) was based on that. In addition, the goal of the bigger project is the development of a comprehensive upper airway model for evaluation of the effect of surgery prior to any surgical intervention.

The goal of this Master's thesis is firstly to present a background of upper airway modelling. An upper airway model consists of a static model of the upper airway and a dynamic component, in this case - airflow. The purpose of the model is to aid prediction of treatment of upper airway disorders prior to any actual surgical intervention. The larger project, of which this thesis is a part of, has the goal of making exactly such a comprehensive upper airway model with which it would be possible to determine the success of surgery (used in this case to treat sleep apnea) prior to surgery. Thus there is a description of sleep apnea in the first part of this document, as it is the target of the bigger project.

The other goal of this thesis is to segment the upper airway system of orthognathic surgery patients, using both pre- and post-operative MR (magnetic resonance) images. This is done due to the fact that the exact effects of the surgery on the upper airway system are largely unknown and, at the same time, it will provide a static model of the upper airway system.

1. Theoretical background

Before the literature review and image segmentation, some theoretical background is presented to help the reader understand the more advanced issues and their interrelations better. Firstly orthognathic surgery, which was performed on the patients, whose MR images were segmented, is described. As the bigger project, of which this thesis is a part of, is mainly concerned with sleep apnea and treatment planning of it, it is followed by a short sleep apnea review, which includes risks that it has, pathogenesis of it (in some cases theories on it, as it is a complex matter) and in addition different treatment options available. It is not aimed to encompass all possible information regarding the

aforementioned subjects, but to provide a comprehensive view of the issues associated with it.

1.1. Orthognathic surgery

Orthognathic surgery refers to a surgical manipulation of the upper or lower jaw. It is a very complex operation and thus takes up about 3 years from initial planning to actual operation (based on the pre- and post-operative image acquisition dates). It is performed for medical (for instance, solution of chewing and speech problems) and cosmetic purposes, and it indeed does change the appearance significantly.

Orthognathic surgery is based on interaction between 3 specialists, that is, a dental practitioner, an orthodontist and a cranio-maxillo-facial surgeon. The general dental practitioner identifies existing orthodontic problems and refers the patient to an orthodontist, who then proceeds to actual treatment planning. (Bill et al. 2006.) The process itself involves an extensive pre-treatment planning, based on clinical and radiological findings, cephalographic information, photostatic information.

However, it is known that it affects the upper airway system too. For example, it may increase the volume of the upper airway. Thus, it is used to treat sleep apnea as well. It also affects the morphology of the associated muscles and skeletal system in a way that is not generally known. It was to be determined in this Master's thesis, whether it is possible to see the effect from volumetric analysis and segmentation of images. As the main focus of the larger project of which this thesis is a part is sleep apnea, a description of sleep apnea follows.

1.2. Sleep apnea

Sleep apnea is a common breathing disorder that occurs during sleep. One can get the view of the prevalence of the condition from the fact that 3% of the children are affected by OSA in USA, meaning millions of children alone in USA. (Donnelly 2010) And that is not counting the adult population, 2-4% of which is said to be affected by OSA as well. (Jordan et al. 2008.)

Sleep apnea can be obstructive, central and mixed (sometimes referred to as ‘complex’). The most common type is OSA or obstructive sleep apnea, which is characterized by repetitive narrowing and/or collapse of the pharyngeal airway (for upper airway anatomy refer to Figure 1.1). (Eckert et al. 2009.) The other type, central sleep apnea (CSA), shows a lack of drive to breathe, thus resulting in insufficient ventilation. Additionally, both of these pathologies can occur simultaneously, this being referred to as complex or mixed apneas. Sleep apneas cause improper gas exchange, frequent catecholamine surges and impaired sleep continuity. (Eckert et al. 2009; Aittokallio et al. 2001) The subsequent blood gas disturbance and arousal from sleep stimulate the sympathetic nervous system resulting in surges of blood pressure. All of

the mentioned consequences impart stress on the cardiovascular system and thus may lead to serious cardiovascular problems In addition, when talking about sleep apnea in children, it can lead to problems such as learning disabilities, attention deficit disorder and failure to thrive. (Donnelly 2010.)

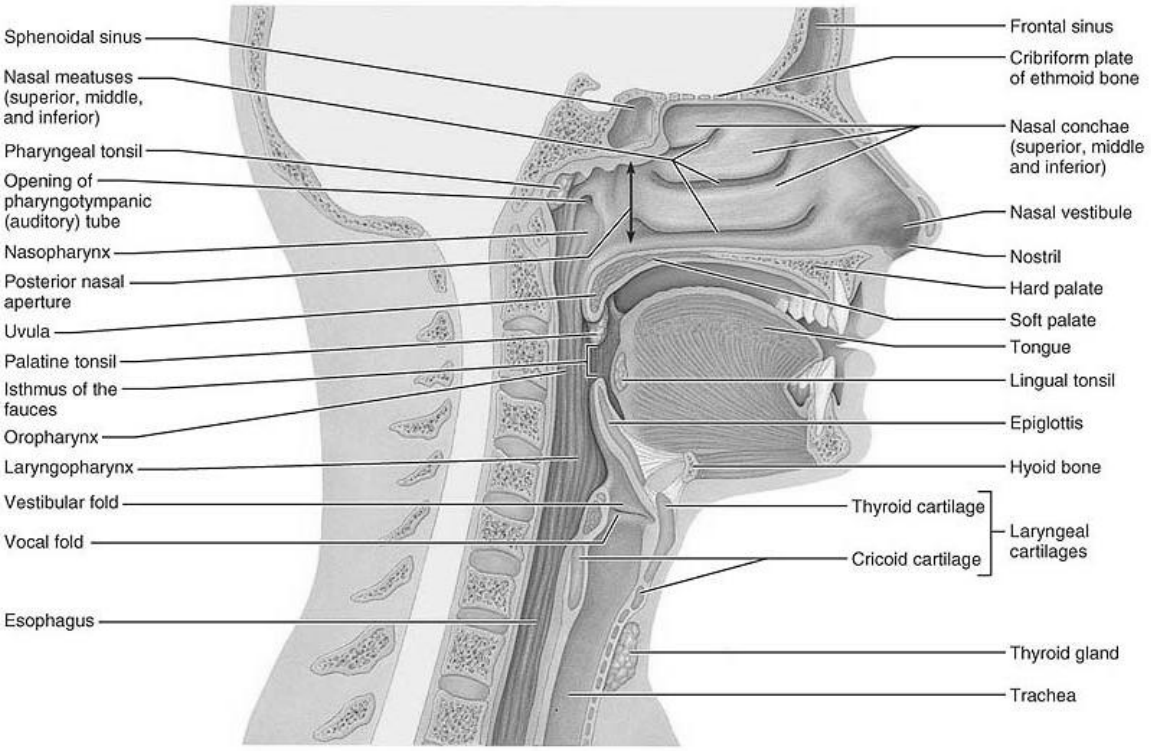

Figure 1.1. *Upper Airway Anatomy. (Marieb & Hoehn 2007)*

OSA is a common disorder. It is characterized by repetitive pharyngeal airway collapse which results in either hypopnea (partially reduced ventilation) or apnea (totally reduced, or absent, ventilation). As a result, hypoxemia (insufficient amount of oxygen in the organism) and hypercapnia (larger than normal concentration of CO_2 in the bloodstream) manifest themselves, despite the patient's continuing efforts to breathe (and stimulate them even further). Despite the continuing efforts to breathe in, the airway is only opened when the patient awakens. Then hyperventilation occurs, in order to restore the blood gas balance, which was disturbed during the (hypo)apnea event. After this, the patient returns to sleep and the event takes place again. Due to the repetitive nature of these respiratory events, sleep is significantly fragmented, causing insufficient amount of sleep. That results in fatigue in wakefulness, and even in neurocognitive dysfunction which impairs the ability of many day-to-day tasks, such as driving a car. In addition to this, the repeated hyperventilation results in great strain on the cardiovascular system, thus potentially causing serious problems in it, especially if the cardiovascular system is not fully healthy before all sleep apnea related events start. (Eckert et al. 2009.) The pathogenesis (or rather theories of it) of OSA is presented in the next section of this thesis. However, it has to be noted, that there is a lack of understanding the pathogenesis even of OSA, not mentioning CSA, which has a much

more complicated mechanism, as the causes of it are neuromuscular. This is largely due to the lack of understanding pharyngeal mechanics via a unifying model, that is able to accurately simulate the pharyngeal collapse with the use of a variety of data. (Xu et al. 2009.)

Contrary to OSA, which is chiefly identified by efforts to breathe in when there are obstructions in the airway, central sleep apnea (CSA) is described by the lack of drive to breathe during sleep. The effect it has is similar to OSA, as it results in frequent (depending on the number of events during sleep) night time awakenings, thus also causing daytime sleepiness and strain on the cardiovascular system. (Eckert et al. 2009.)

Mixed (complex) apneas are a combination of obstructive and central apneas, meaning that it consists of a complete pause of respiration, shortly followed by an obstructive respiratory effort. In fact, even though CSA and OSA are often separated in their description, frequently they overlap and occur simultaneously in patients. (Eckert et al. 2009.) Central apenas might lead to upper airway closure, which in turn may be connected with OSA, in a way that there is reduced drive in all dilator muscles. Mixed apneas can in general be described by the percentage of CSA vs. OSA that the patient has (figure 1.2). Furthermore, it has been observed that after commencing CPAP (continuous positive airway pressure, described in the following chapter in more detail) treatment, patients develop CSA symptoms when they previously had only OSA, meaning that when the airway collapsibility is reduced, the patient's apnea shifts more to the CSA side.

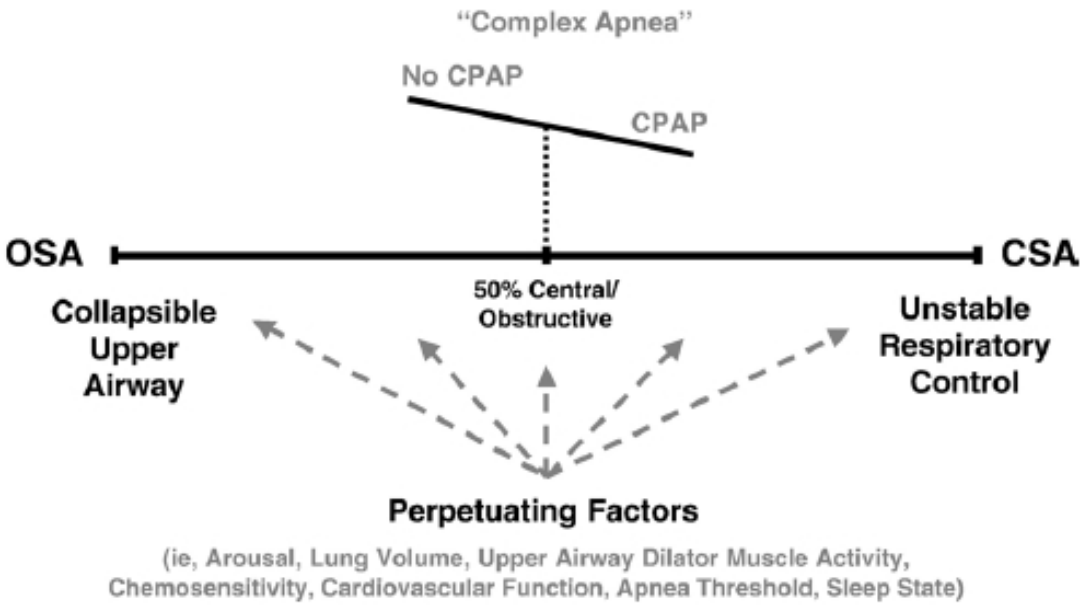

Figure 1.2. *The mixed apnea spectrum and underlying factors. (Eckert et al. 2009.)*

Normally sleep apnea can be partially self-diagnosed due to obvious symptoms, such as frequent night arousal, and others, described above. In addition, sleep studies using polysomnography can be performed and then the severity of the condition is determined analysing the upper airway anatomy using some imaging modality, usually

CT or MRI. Azarbarzin & Moussavi conducted a study analysing the sounds that snorers make and tried to associate them with the severity of obstructive sleep apnea. For that data (snoring sounds recorder over the suprasternal notch of trachea) from 42 snorers, including 15 non-OSA subjects, while the remainder were diagnosed with variously severe OSA (starting from hypopnea, going to quite sever cases). This study concluded, that the largest amount of snoring sounds were made by non-sleep apnea snorers, while ones with hypopnea made less but higher pitched sounds and finally the severe OSA patients did not induce many sounds. This is explained by the fact that when the airway is obstructed completely no snoring occurs. Azarbarzin & Moussavi 2009.)

1.2.1. Pathogenesis of sleep apnea

The major pathology in sleep apnea patients is a collapsible pharyngeal airway. While in healthy subjects the narrowest and most collapsible region is the nasal cavity, the velopharynx is considered to be the most collapsible region of the upper airway and the most flow-limiting structure during sleep in OSA patients. (Jeong et al. 2006.) As velopharynx is the narrowest region of the pharyngeal airways, it is continuously exposed to local increases in airflow speed and decreases in intraluminal pressure, which may well play a very significant role in airway occlusion and the pathogenesis of OSA. (Jeong et al. 2006.) Collapsibility of a particular airway can be described by P_{crit}, critical pressure when the airway collapses. In healthy people it is negative, while in OSA patients it is zero or positive. A lengthened pharyngeal airway and a reduced velopharynx to hypopharynx cross-sectional are ratio contribute to pathogenesis of OSA, while nasal obstruction may further accentuate OSA symptoms. (Jeong et al. 2006.) One other important factor in the cause of a collapsible pharyngeal airway is fat deposition around it. Thus obesity often is the cause of sleep apnea. There are other anatomical factors, that can cause pharyngeal airway collapsibility: airway length, tongue volume and lateral pharyngeal wall thickness. (Eckert et al. 2009; Aittokallio et al. 2001)

However, anatomical abnormalities amount only to one side of the problem and do not fully explain it: if they were the sole cause of sleep apnea, it would also occur during wakefulness and in all sleep stages, while it has been observed, that OSA is more severe during rapid eye movement (REM) sleep than in non-REM sleep and in stage 2 compared to slow wave sleep. (Jordan et al. 2008.) It was also reported, that most OSA patients have some periods of sleep without repetitive apneas or hypopneas. (Jordan et al. 2008.) which indicates that patients overcome the abnormality in some way for some time. This was shown to be largely due to the significantly increased activity of the genioglossus muscle. (Jordan et al. 2008.) One other cause is the upper airway dilator muscles, of which there are several different, and they all are much more active during wakefulness, especially if healthy control subjects are compared with OSA patients, who exhibit an increased activity in the dilator muscles during wakefulness. (Jordan et

al. 2008.) They dilute or stiffen the upper airway. The biggest and most recognized upper airway dilator muscle is the gengioglossus which is a part of the tongue. (Aittokallio et al. 2001; Donnelly et al. 2010)

Lung volume or rather the reduction of it during sleep can be one other OSA pathogen. (Shin et al. 2013.)

The central nervous system, which regulates the breathing, can also be the cause of sleep apnea. Ventilator control is an important factor to consider as well, especially when the patients don't respond to maxillomandibular advancement (MMA). (Shin et al. 2013.)

The diagnosis and analysis of sleep apnea used to be done primarily with the help of polysomnography (Farré et al. 2008; Susarla et al. 2010), but recently use of special sleep MRI modalities has been used. (Donnelly 2010; Shin et al. 2013.)

Alcohol consumption and smoking also contribute to sleep apnea. Smoking damages the upper airway, not only lungs, in causing chronic inflammation and damage to the upper airway thus increasing its collapsibility. Alcohol is known to relax the upper airway dilutor muscles and in so doing the collapsibility of it is increased as well. Alcohol consumption can thus prolong apnea episodes, suppress arousals and increase the frequency of apnea episodes. However, the mechanism of this is not fully understood. (Lam et al. 2010.)

1.2.2. Treatment of sleep apnea

There are various ways to reduce the severity of sleep apnea or even to treat it completely just by changing one's lifestyle to a healthier one. For instance, even slight weight loss might alleviate the apnea. In addition, smoking and alcohol might contribute to sleep apnea. However, quite often it is necessary to treat the apnea medically and there are several ways to treat it. The treatment is can be an external breathing device, certain medications, a dental device an orthodontic device or surgery. (Simon & Zieve 2012; Flemons & McNicholas 1997)

One of the most common ways to treat sleep apnea is continuous positive airflow pressure (CPAP). It was introduced in the early 80s, first devices being quite bulky and noisy, but the innovation was swift.

It involves applying a continuous stream of air via a mask during sleep, thus inhibiting the airflow collapse. The standard CPAP machine delivers a continuous airflow, but there are variations (Simon & Zieve 2012.):

- Autotitrating positive airway pressure (APAP), which detects changes in the breathing pattern and adjusts the airflow accordingly
- Bilevel positive airway pressure, which delivers air in two different pressures (a larger one for inhaling and a smaller one for exhaling)

Medications in sleep apnea are not very effective, except in special cases and certain medicines, namely:

- Modafinil (Provigil) is sometimes used to reduce sleepiness caused by sleep apnea, but only in addition to CPAP
- Thyroid hormone can help patients with sleep apnea who also have low thyroid levels (hypothyroidism)

Dental devices help with light to moderate sleep apnea. They have to be custom made by a dental specialist and need constant care and adjustments. Additionally, they involve some unpleasant effects, such as saliva build up, soreness and permanent change in the position of teeth and jaws. There are two main kinds of them (Simon & Zieve 2012; El et al. 2011):

Mandibular advancement device (MAD), which resembles a sports mouth guard and forces the lower jaw forward and down slightly, keeping the airway open.

Tongue retaining device (TRD), a splint device, that holds the tongue in place to keep the airway as open as possible

There is an orthodontic treatment, called rapid maxillary expansion that involves a screw device, applied to upper teeth and tightened regularly. This helps to reduce intranasal pressure. (Simon & Zieve 2012.)

Surgery is the last resort in treating sleep apnea and is used in severe cases of it. In addition to this, it's success rates are quite modest. (Simon & Zieve 2012.) One reason of non-satisfactory success rates of surgery is that it is imperative to know the exact obstruction point in order for the surgery to be effective, but this has proven to be a rather elusive goal. (Wang & Elghobashi 2013.) In general, a common type of surgery used is uvulopalatopharyngoplasty (UPPP). (Simon & Zieve 2012.) During this surgery all or part of uvula, soft palate and throat tissue is removed. In addition, tonsils and adenoids are removed too, if they are present. This increases the width of the upper airway, improves the movement of the soft palate and prevents some of the muscles active in upper airway collapse from functioning, thus alleviating sleep apnea. A lot of painful and unpleasant complications, such as infection, mucus in the throat, impaired sense of smell, regurgitation of fluids through nose or mouth, changes in voice frequency and difficulty in keeping liquids out of the airway. There are other less common and case specific methods, than include (Simon & Zieve 2012.):

- Laser-Assisted Uvulopalatopharyngoplasty (LAUP)
- Pillar Palatal Implant implantation
- Tracheotomy
- Maxillomandibular advancement (MMA)
- Genioglossus (tongue) advancement
- Hyoid advancement surgery

- Surgery of nasal obstructions, if present

Often it is uncertain how the patient will react to a certain treatment. Thus it is very useful to have a model to predict how a surgery, for example, will influence airflow in the upper airway.

When talking about sleep apnea in children, one of the most common paediatric surgeries performed is adenoidectomy and palatine tonsillectomy related to OSA. (Donnelly 2010.)

2. Modelling of airflow in the upper airway

First of all, it has to be said, that there is a lack of a unifying upper airway model, that could simulate the airflow in the upper airway using different incorporated data. (Xu et al. 2009) The current theoretical models include the Starling resistor model (described in one of the sections of this chapter) and the balance of forces model, which predicts the negative imbalance between muscles, that dilate the upper airway and forces that collapse the airway, which results in OSA in patients. These models, however, do not take into account the various anatomical structures associated with the upper airway and their properties. (Xu et al. 2009.) Thus there is a need of an all-encompassing comprehensive model.

Currently, properties of airflow in the upper airway are not fully understood because of the complex and highly patient-specific geometry of the airway, flow transition (from laminar to turbulent) and flow-structure interaction during breathing. A significant factor, additionally, is the lack of actual clinical data of velocities of air during breathing in different points of the upper airway. (Wang & Elghobashi 2013.)

The flow in the upper airway undergoes transition from laminar to turbulent and reverses its main direction about every two seconds. (Wang & Elghobashi 2013) Due to this, curved streamlines, recirculation regions, secondary and jet flows result. In order to predict airflow in the upper airway accurately, the chosen model has to be able to simulate low Reynolds number turbulent airflow in the complex structure of the upper airway.

It is necessary not only to image the upper airway using some imaging modality, most commonly MRI or CT (computed tomography) and make the upper airway model based solely on it, the static component, but also to have a functional, dynamic component. This means simulating airflow in the upper airway model using some sort of modelling. The most common ways to do this are based on Computational Fluid Dynamics, or CFD (Cheng et al. 2013; Zhao et al. 2013; Xu et al. 2006; Iwasaki et al. 2011; Wang et al. 2009; Jeong et al. 2007; Ito et al. 2011; Mylavarapu & Shanmugam et al. 2009; Mylavarapu & Mihaescu et al. 2009; De Backer et al. 2007; Sung et al. 2006; Persak et al. 2011; Sarasen et al. 2012; Mihaescu et al. 2008;) (the majority of studies in the field were done using this method), using finite element modelling (FEM) (Huang

et al. 2013; Xu et al. 2009; Xu et al; Yu et al. 2009) and Large Eddy Simulation (Mihaescu et al. 2011; Mihaescu et al. 2011) (which is a method in CFD, but will be described separately in greater detail nonetheless). CFD and FEM are more of umbrella terms for the studies reviewed, as they themselves employ different methods in the studies, for example, CFD studies may employ one of the following methods: Reynolds-averaged Navier-Stokes, Large Eddy Simulation or Direct numerical simulation. (Wang & Elghobashi 2013) There are various other approaches and studies too.

One step, common for all methods, is acquiring the structural (sometimes also referred to as "static") model using an imaging technique, usually CT or MRI and image processing (including segmentation) software. The other step is to actually add dynamics to the model, using airflow modelling and tissue behaviour modelling with appropriate modelling software. Generally speaking, the goal is to link airway anatomy with airway physiology into a comprehensive model. Below different approaches in upper airway modelling are described, using examples from existing studies done in the field.

2.1. Computational fluid dynamics (CFD)

Computational Fluid Mechanics have been successfully used in traditional engineering for a long time. Recently, it has been used in upper airway studies, usually by combining CFD with either MR or CT imaging to construct a detailed anatomical upper airway model. It has gained popularity due to its capability to predict fluid flow characteristics non-invasively, when input flow variables (for example expiratory/inspiratory flow rate, breathing rate, input flow turbulence and lung pressure) vary. It has the advantage over in vivo, in vitro and mechanical experimental models in that using CFD different flow variables and flow forces can be inspected in great detail. (Mylavarapu et al. 2009.)

CFD is a means of adding airflow and pressure profiles to a static image (whether it be MRI or CT). As one of the most important things to consider in CFD is the type of airflow taking place in the actual airway, it has to be taken into account carefully. Of particular importance is the transition of laminar flow to turbulent flow when there is an occlusion and during the process of upper airway collapse. That is based on solution of the Navier-Stokes equations (De Backer et al. 2008.):

$$\frac{\partial \overline{u_i}}{\partial x_i} = 0; \tag{1}$$

$$\frac{\partial \overline{u_i}}{\partial t} + \overline{u_i}\frac{\partial \overline{u_i}}{\partial x_j} = -\frac{1}{\rho}\frac{\partial p}{\partial x_i} + \frac{\partial}{\partial x_j}\left[(\nu + \nu_\tau)\left(\frac{\partial \overline{u_i}}{\partial x_j} + \frac{\partial \overline{u_j}}{\partial x_i}\right)\right]. \tag{2}$$

Where $\overline{u_i}$ is time averaged velocity in three Cartesian directions (x, y, z), p is the time averaged pressure and ρ and ν are the density and kinematic viscosity of the fluid,

respectively. These equations, in turn, are based on three fundamental principles, namely:

1. Mass can neither be created nor destroyed;
2. Force equals the time rate of change of momentum;
3. Energy can't be created or destroyed; it only changes form.

The equations can be solved either in a two dimensional (2D) or three dimensional (3D) domain. To do that, dimensions, or boundaries are required. Hence the CT or MRI images of the upper airway. They provide the required data for the computation of the equations. However, they first need to be divided into small components in order for the computation to take place, thus forming a computation grid. Flow parameters, such as flow velocity, pressure and density are calculated in each of the grid elements. Preliminary knowledge of the airflow allows the grid density to be uneven: there can be more elements where the flow gradient is greater for a more accurate model and fewer grid elements where the gradient is low. This is necessary because if the grid is too dense, it will cost too much (computer and hence time resources) to compute the model. A typical upper airway model can have anywhere between 500000 to 1600000 grid elements, depending on the volume of the upper airway. (De Backer et al. 2008.)

An important choice that researchers have to make is what type of flow to choose in the modelling process. That depends on Reynolds' numbers and the type of airflow, but it has to include both laminar and turbulent airflow for accuracy. The Reynolds number, *Re*, varies from 800 in light breathing (200 ml/s) to excesses of 9300 in heavy breathing (100 l/min) in the trachea. (Jeong et al. 2006.)

Mylavarapu et al. (Mylayarapu et al. 2013.) conducted an interesting study, in which virtual surgery is used. The patient has glottic and subglottic stenosis, not sleep apnea, but the airway modelling is essentially the same. The surgeon "operates" on a reconstructed airway model, modifying the pre-treatment airway boundaries so that they reflect the changes to be done in a coming surgery. Then CFD is used to evaluate the virtual post-operative airflow. It is then compared to the baseline airflow model done beforehand to assess the efficiency of the surgery both qualitatively and quantitatively. However, this requires a very accurate model of the upper airway. The model was reconstructed from 83 CT axial scans, each slice being of 3mm and 512x512 pixels, with a pixel spatial resolution of 0.49mm. The reconstruction itself was done with medical imaging software MIMICS (Materialise, Belgium). It is also important to define boundaries of different tissues in the model. This was done by setting a threshold value on gray scale intensity of different tissues: airways appear as black, surrounding soft tissues as grey and bone as white. This means grouping voxels in Hounsfield unit ranges of interest (black, representing air, being nearly 1000 HU) into a mask, from which the raw 3D model is generated by triangulation. After that the raw model is remeshed, improving its quality by smoothing the surfaces and edges. Next the final mesh is generated, using Gambit (Ansys, USA) software. Due to insufficient nasal

cavity image quantity, it is not generated and considered in this study. (Mylayarapu et al. 2013.)

Zhao et al. (Zhao et al. 2013.) used CFD to construct a model that predicts patient response to MAS (mandibular advancement splint), sometimes used in treating sleep apnea. There were 7 patients, with known response to MAS treatment (some responsive, some partially, some non-responsive). The goal was to see, if modelling can help predict the outcome of the treatment, because it is currently hard to tell before the treatment if the patient will respond or not, and thus can lead to waste of resources in the case of a patient not responding to the treatment. For this purpose, upper airway physical models, generated by means of rapid prototyping from MRI images from awake patients in the supine position, both with and without MAS and generalized upper airway flow and pressure profiles were used to determine whether there is a relationship to treatment outcome. By this viability of prediction based on computational methods would be increased. MAS treatment outcome could be predicted based on patient-specific geometries (achieved from an imaging modality) alone. Clear and reliable results were achieved, namely, there was clear correlation between the simulated data with the known treatment outcomes of the 7 patients, who had varying responses to MAS treatment. The upper airway model in this study does not include the nasal airway.

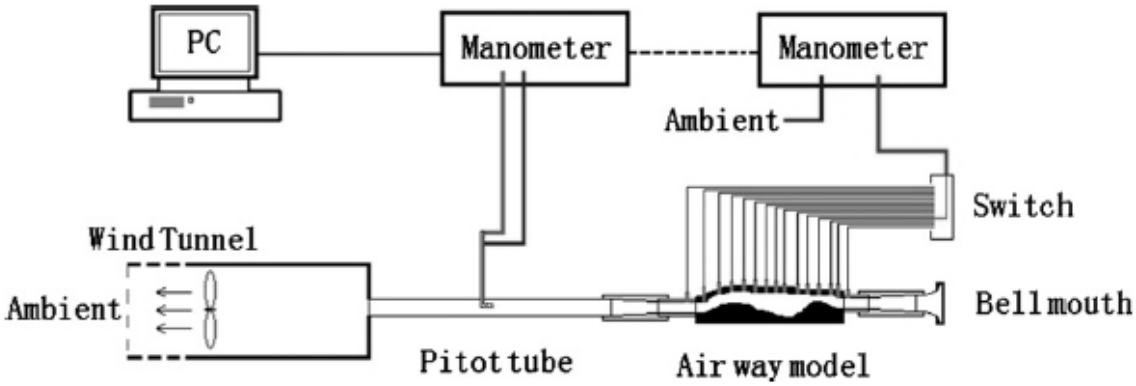

Figure 2.1. *Experimental setup used in the study of Zhao et al. (Zhao et al. 2013.)*

In the study of Xu et al. (Xu et al. 2006.) CFD is applied to study the effect of airway geometry on upper airway pressure and flow resistance in children with sleep apnea. The CFD predictions were validated using a scaled rigid model. In image acquisition, MRI studies were performed on 3 children. There was a control model (from a healthy individual) as well as a model from a sleep apnea patient. The models of Xu et al. also include nasal airways. Their experimental setup can be seen in figure 1.4, where A is the block diagram of the experimental setup, B - a piston air pump for airflow production, C - a transparent rigid airway model, produced by rapid prototyping, D - flow measured at the inlet, E - p(t) (pressure depending on time) measurements at location 3, the maximum narrowing point and F - flow rate vs. time for unsteady flow.

A software package based on 3DVIEWNIX was developed by the Medical Image Processing Group of University of Pennsylvania and used for various image processing operations needed to construct 3D models from the MRI images. Both the computational and mechanical models raised the possibility, that narrowed segments of the pharynx may not receive significant positive pressure, compared to negative pressures in inspiration. The study concludes, that are restriction in the pharynx may be as important as nasal resistance in airway collapse. Thus, it is concluded, that upper airway models might benefit from adding pharyngeal restriction in addition to airway collapse properties.

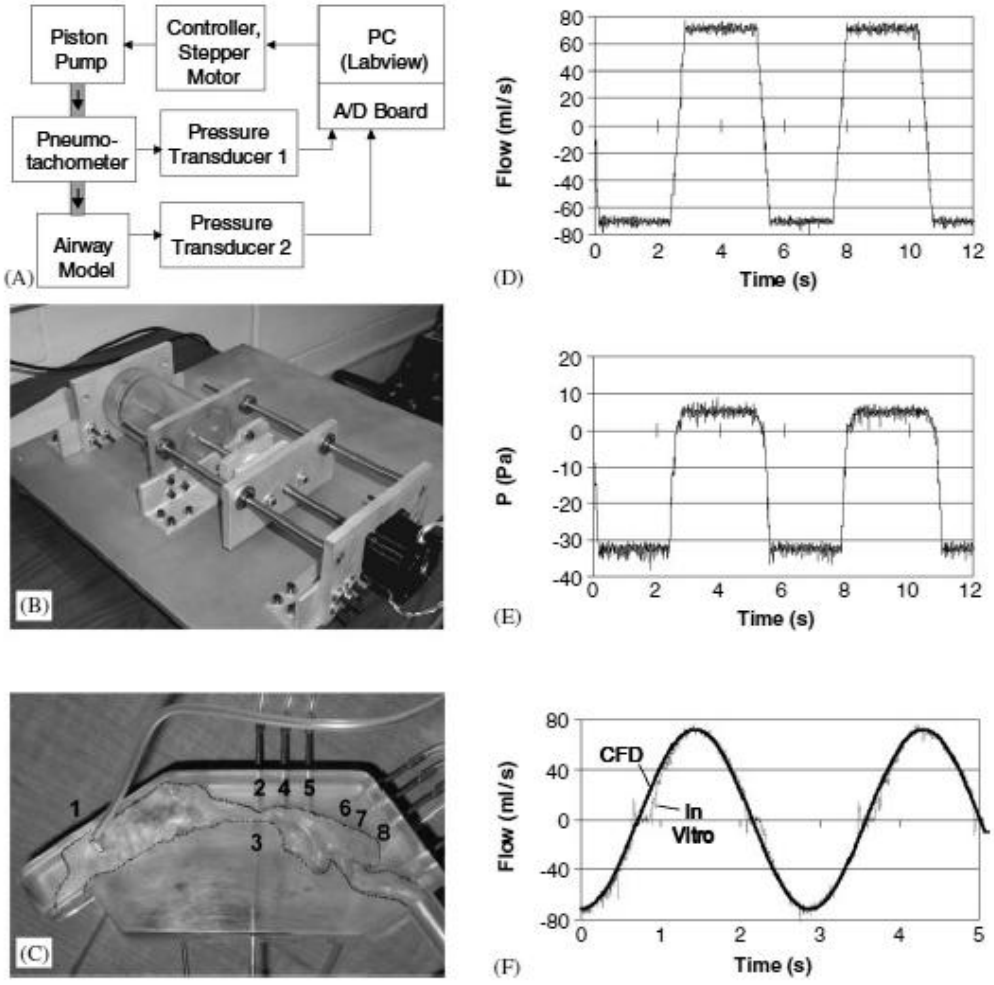

Figure 2.2. *Experimental setup used in Xu et. al study. (Xu et al. 2006.)*

Van Holsbeke et al. used CT to reconstruct upper airway models in patients (in this case, children) in three dimensions. CFD was used to model low inspiratory airflow in the reconstructed structures using open source software (SnappyHexMesh 2.0.1, OpenCFD Ltd, UK; OpenFOAM 2.0.1 OpenCFD Ltd, UK). The patients first underwent polysomnography and a clinical assessment of upper airway patency. The CT scan was performed while awake. It was reported, among other things, that children

with OSA had a significantly lower minimal cross-sectional area at zone 3 than healthy subjects. (Van Holsbeke et al. 2013.)

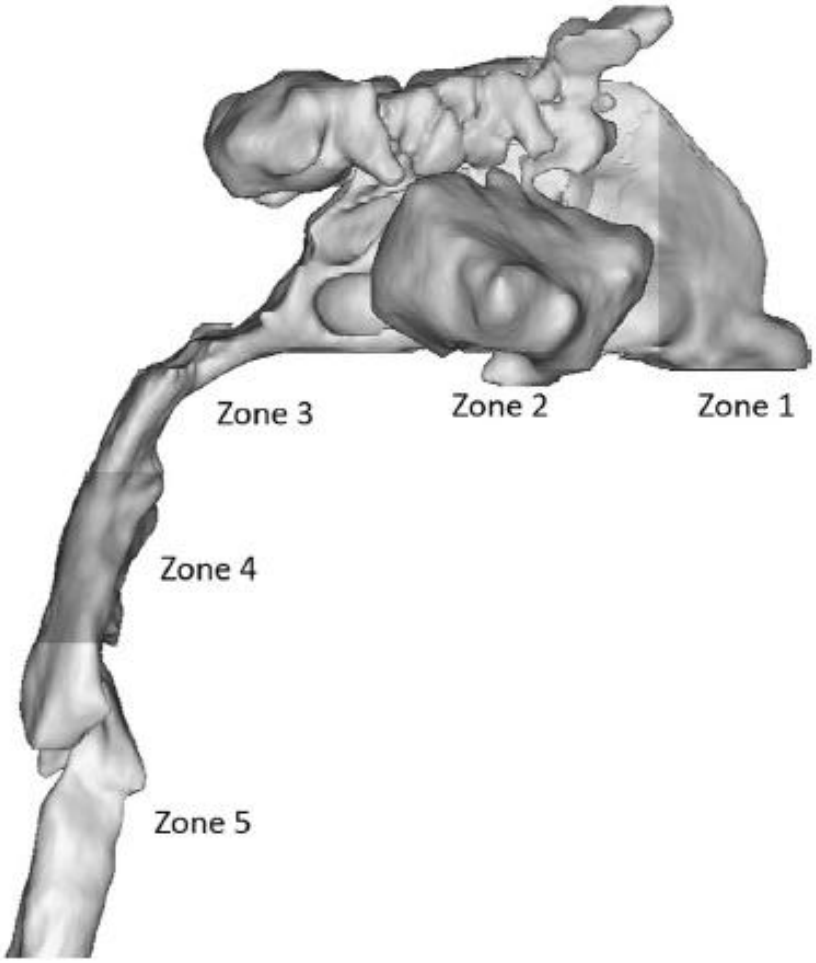

Figure 2.3. *Upper airway model with zones 1-5 used in Van Holsbeke et al. study. (Van Holsbeke et al. 2013.)*

Iwasaki et al. use fluid mechanical computation to simulate airflow to detect defects in the upper airway and cone beam CT images to acquire the shape of it (fig. 1.6, A and B show the acquisition of the airway shape with CBCT (cone beam computed tomography) and C and D show the airflow simulation, with D having different colour coded pressure regions, red being higher, blue - lower pressure). It investigates 40 children with dolichofacial and brachyfacial malocclusion. The conclusions of the study are that most of the children had airway obstructions in different sites of the upper airway, including the nasal cavity, nasopharynx, oropharynx and hypopharynx. (Iwasaki et al. 2011.)

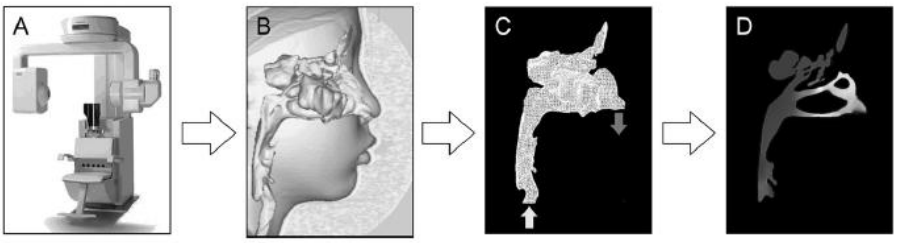

Figure 2.4. *FMS (Fluid mechanical simulation) system used in Iwasaki et al. (Iwasaki et al. 2011.)*

De Backer et al. reconstructed upper airway geometric models from CT data sets as computational meshes (triangular meshes for the upper airway meshes and hybrid meshes inside) to analyze the dynamics and behaviour of the human respiratory system. The main idea of this paper is that it is possible to predict the chances of success of Maxillomandibular Advancement treatment by analyzing anatomical airway changes using 3D geometrical reconstructions and CFD modelling.

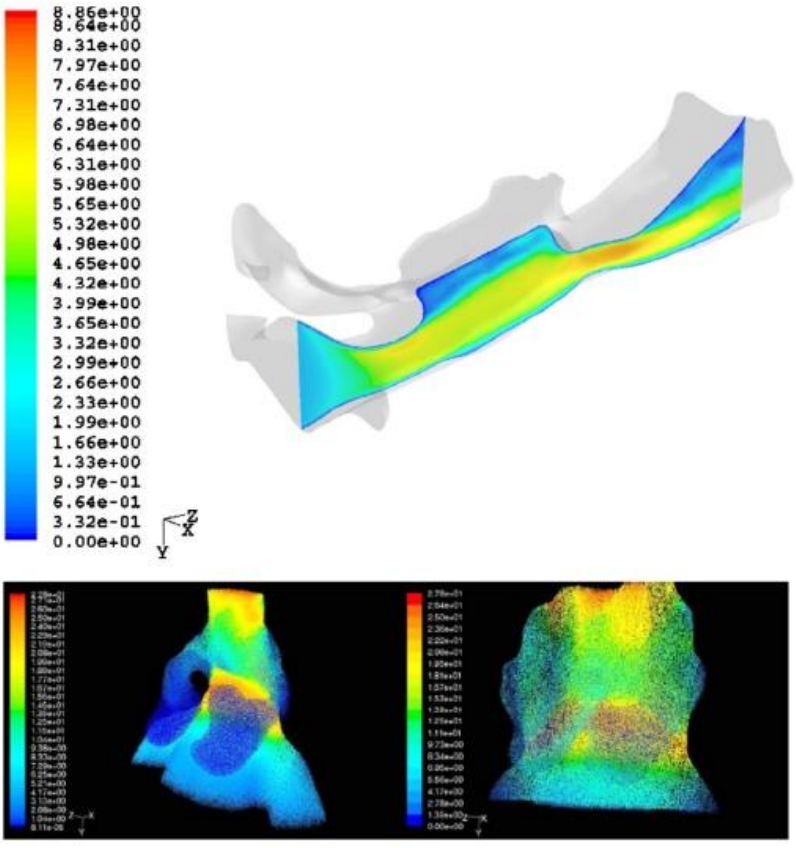

Figure 2.5. *Velocity contours inside upper airway of SBD patient (upper) and velocity intensities inside the upper airway without (left) and with the MAD (right) (De Backer et al. 2007.)*

It is assumed in this study that the airways are rigid, which is not the case in reality, as they are surrounded by muscles and soft tissue and can be deformed in various ways. (De Backer et al. 2007.)

Mylavarapu et al. (Mylavarapu et al. 2009.) performed a study, in which the goal was to validate CFD computations. As there was no accurate invasive clinical flow measurements, the approach chosen was that of a mechanical model, that is, to use experimental flow data from that model. The physical model was constructed from MR data of a 17-year-old adolescent with a BMI index of 26 kg/m^2. The axial T1 weighted MR data was used firstly to construct a CAD model of the upper airway, using commercial medical imaging software MIMICS® (Materialise, Belgium). The initial acquired poly line boundaries are smoothed and re-meshed with REMESHER, which is a module of the MIMICS software. Then a 3D upper airway is reconstructed, and finally an experimental model is made. The experimental model is 2 times larger than the actual upper airway for better accessibility. The 2:1 scaled mechanical upper airway model was constructed using Stereo Lithography process using SLA resin (Somos Watershed 11,110) material which yielded nearly uniform airway wall thickness. For measurement of pressure in different points of the upper airway model, pressure ports were created (figure 2.6).

The resulting data was compared with several different numerical approaches of CFD, which were available within the FLUENT commercial software framework. Unsteady Large Eddy Simulation (LES), steady Reynolds-Averaged Navier-Stokes (RANS) with two-equation turbulence models (namely k-ε, standard k-ω, and k-ω Shear Stress Transport (SST)) and with one equation Spalart-Allmaras model. From all these approaches the standard k-ω turbulence model compared best with the static pressure measurements using the mechanical model, with an average error of about 20% over all ports. The highest positive pressure was observed in the retroglossal region below the epiglottis and the lowest negative pressure was recorded in the retropalatal region. The largest pressure drop was at the tip of the soft palate, as it has the smallest cross section of the airway. (Mylavarapu et al. 2009.)

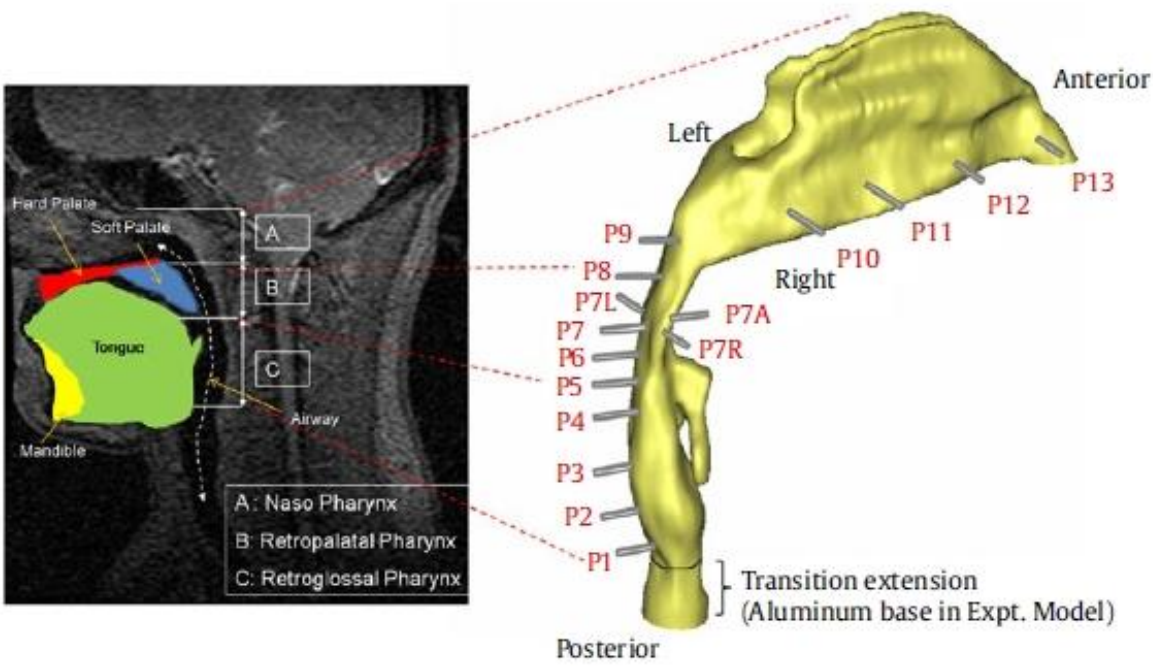

Figure 2.6. *The 3D model of the upper airway and locations of the pressure ports for measurement of the desired data in the study of Mylavarapu et al. (Mylavarapu et al. 2009)*

In one already described study (in the beginning of this section), Zhao et al. (Zhao et al. 2009.) performed a study, which had the goal of predicting patient response to mandibular advancement splint treatment. The study of Cheng et al. (Cheng et al. 2013.) had the goal of assessing the effects that maxillomandibular advancement surgery has on sleep apnea patients. Their hypothesis was that the cure of obstructive sleep apnea by maxillomandibular advancement surgery can be predicted by analyzing the effect of anatomical airway changes on the pressure effort required for normal breathing. (Cheng et al. 2013.) For that a 3D numerical model of the upper airway was used. The model consisted of a 3D static (geometric) model from CT data, which was acquired with the help of image segmentation using open-source libraries, Insight Segmentation and Registration Toolkit and Visualization Toolkit, mixed element mesh generation of the numerically constructed airway geometry for discretizing the domain of interest and CFD simulations for flow field prediction and visualization of the degree of breathing obstruction. The paper states that the geometry extraction and manipulation process are the most time-consuming and labour-intensive parts, because of low resolution CT data sets compared to the actual complexity of the human nasal cavity structure. (Cheng et al. 2013.) It is further stated that an airway can be very narrow at the pharynx and that however it should not be closed for calculation of pressure efforts, as many of the OSA patients airways collapse at the end of exhalation when in a supine position in the CT scanner. It is also important that the patient's head is in the same position for the pre- and post-operative image sequences, as the airway geometry is dependent on the position of the head.

The slice thickness in the CT data sets in the study of Cheng et al. varies from 1,25 mm to 3 mm, most being 2,5 mm thick. That is not adequate for acquisition of detailed meshes of the upper airway, because the nasal cavity and part of the upper airway geometry is rather complex.

The study of Cheng et al. used data from 10 patients with mild-to-severe OSA cases. Airflow in pre- and post-operative models was simulated using CFD. A short upstream section was added to the models presented in figure 2.7 below to include the effect of air entrance to the nostril. Furthermore, a straight section of the airway (having a length of 10 times the airway exit diameter) was artificially included to the downstream of the computational domain in order to avoid the flow reversal at the exit plan. A flow rate of 700 ml/s was used (an averaged volume of air for one normal inspiration in adults) was used to calculate the speed of air entering the nose, and the input pressure was set at 1 atm (10^5 Pa), which is the normal ambient pressure. The surgical outcome is measured with the help of ΔP, which is the difference between the pressure at different locations along the airway and the pressure at the cross-section with the base plane through the hard palate, which is required to counter airflow resistance. It was anticipated that the same amount of air inspired requires less pressure effort in the post-maxillomandibular advancement surgery models, due to increase in the airway diameter and volume. It was concluded, based on the CFD simulations, that 1) higher degrees of airway obstruction require more pressure efforts to inspire the normal amount of air, that 2) the pressure effort before the surgery was larger, except in one case, which was due to irresponsiveness to the surgery, that 3) the extent of pressure effort reduction depends on the severity of airway obstruction and the increase of airway space and volume after surgery and 4) that pressure efforts calculated from turbulent flow simulations are larger than those from laminar flow simulations, which is because turbulent airflow causes additional resistance. (Cheng et al. 2013.)

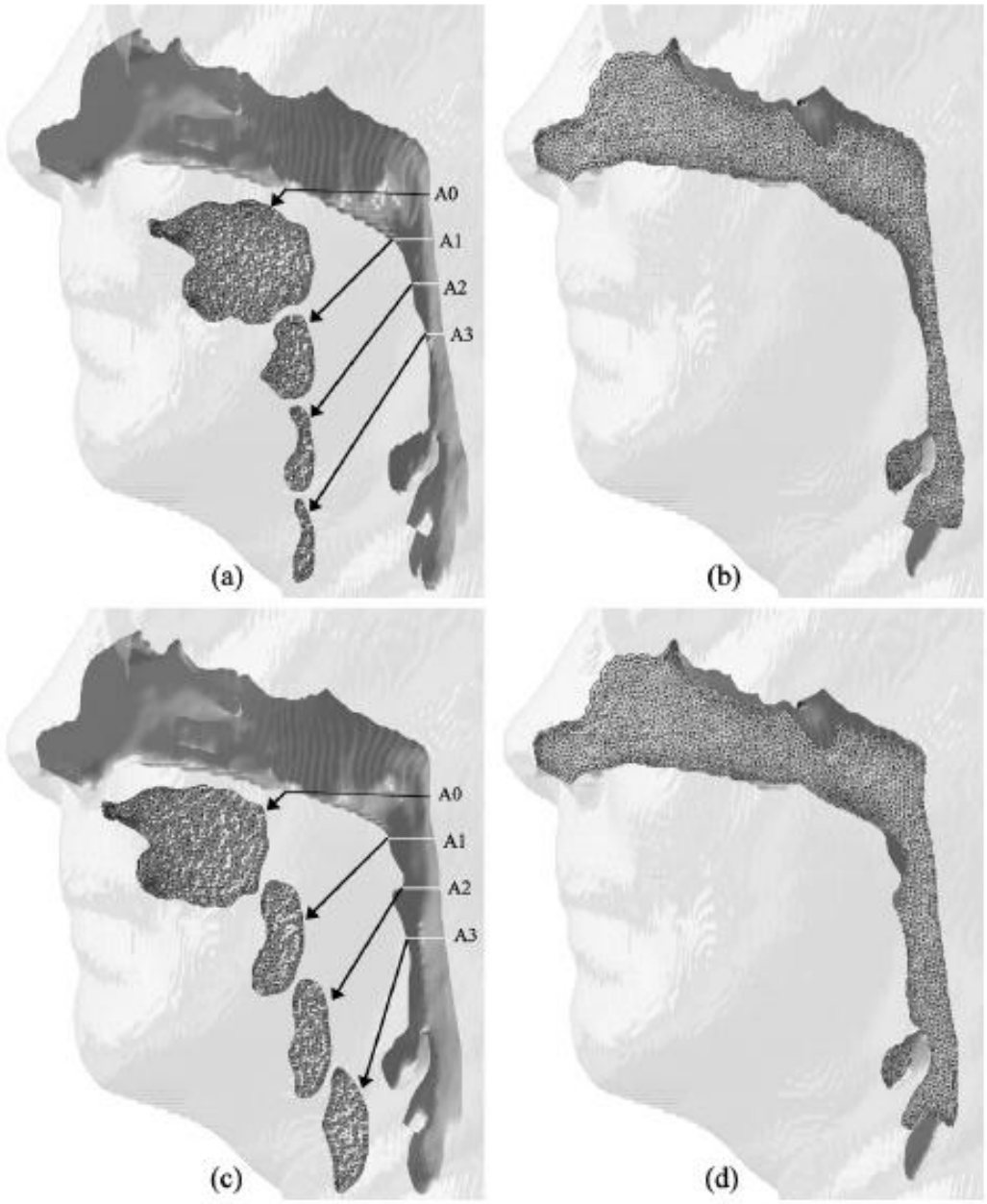

Figure 2.7. *Comparison of geometries and cross-sectional meshes for Case 1, a and b - pre-operative and c and d - post-operative views (Cheng et al. 2013)*

One more attempt to simulate the airflow in the upper airway to predict the outcome of MAS (mandibular advancement splint) treatment was made by Zhao et al. (Zhao et al. 2013). Their approach was to analyze upper airway occlusion and flow dynamics in OSA using the fluid-structure interaction method (FSI). For this purpose images of a known MAS treatment responder were acquired one series with the MAS, another series without, from which respective computational models of were reconstructed. It is claimed in the paper, that this study is the first so far to use a deformable upper airway structure and inspiratory airflow in the study of airflow dynamics. The computational data was validated by a physical experiment on a real scale model, which was constructed using 3D stereolithography.

For computational model reconstruction T1 weighted upper airway scans were obtained with and without the MAS, which was supposed to represent pre- and post-operative conditions. Amira 5 (Visage Imaging, USA) commercial software was used to import the acquired data and segment the upper airway volume. A vertex averaged smoothing algorithm was then applied. Significant increase in volume of the upper airway when comparing the volume with and without the MAS was observed (namely, increase from 12,5 cm^3 to 16,3 cm^3). (Zhao et al. 2013.) The fluid equations were solved using ANSYS CFX 13.0 (ANSYS, USA), with the same boundary conditions used for pre- and post-treatment models. The inspiratory flow rate was modelled as sinusoidal, with a maximum flow rate of 166 ml/s which occurred at 1s. (Zhao et al. 2013.) A static ambient pressure was applied to the nasopharynx as well, as is common practice in this type of simulations. The upper airway tissue was defined as a homogeneous elastic material with a Young's modulus of 7,54 kPa and a Poisson's ratio of 0,45. That in itself is a gross approximation, due to the inhomogeneous and non-liner elastic nature of biological tissue. The FSI simulations were said to have been performed on a 48 core super computer and took 15 days, including the data post-processing work to complete. The computational FSI method was then validated using a physical experiment. For that a flexible model of the upper airway was manufactured using stereolithography from the constructed models. The SLA material had a Young's modulus of 325 kPa and a Poisson's ratio of 0,306, which were determined with the help of tensile testing. The wall movements during simulation were recorded using a high speed camera. In addition, the FSI simulations were repeated with the same conditions as the actual physical model, due to the fact that the material properties varied significantly. For simulation of airway collapse, a flow rate of 500 ml/s was generated. There was a mismatch in the boundary deformation graphs of the computational and mechanical simulations which was allegedly caused by a fabrication error in the physical model production. There was a difference between the results when the model collapsed as well, with the experimental results showing a more inward movement of the tongue base area. The occlusion events at the left posterior oropharynx and anterior hypopharynx were present in both studies. The results overall match quite satisfactorily, with a maximum discrepancy of 0,7 mm (of the wall movement), at the flow rate of 434 ml/s (figure 2.8 below). Contact between anterior and left side retroglossal walls occurred at 0,56s and a flow rate of 127 ml/s before the MAS treatment. This shows a lateral wall initiated occlusion occurring at the base of the tongue. The maximum deformation was 5,81 mm (at the left posterior side of the orophanrynx). With the MAS in place, upper airway deformations were significantly reduced. This corresponded with the actual situation with the patient, who had severe OSA before the MAS treatment and no OSA symptoms thereafter.

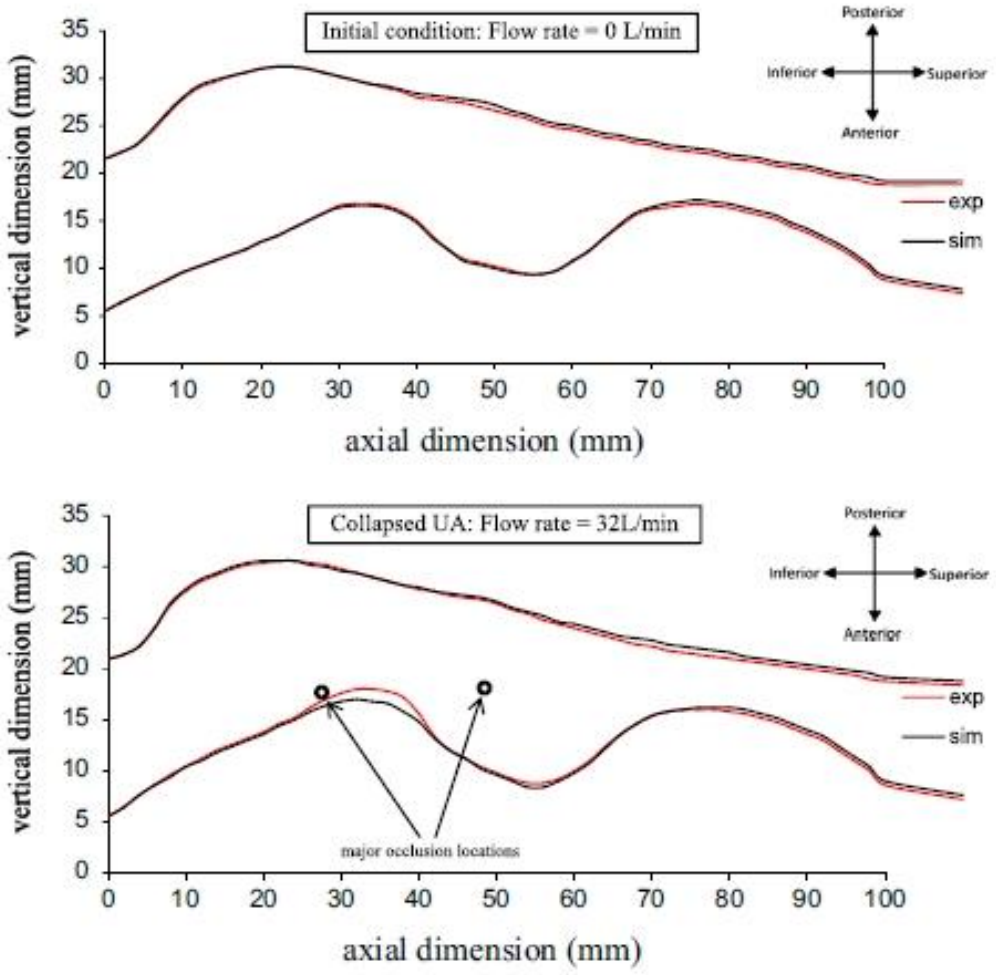

Figure 2.8. *Deformation curves for the FSI simulation (black) and the physical simulation (red) for normal conditions (upper part) and collapsed airway (lower part) (Zhao et al. 2013.)*

Jeong et al. in yet another CFD study use raw data from 3D CT upper airway scans of an OSA patient to construct a CFD model. As for the choice of airflow modelling, Jeong et al. chose the low Reynolds number *k-ε* model, which they claim to have validated using previous literature.(Jeong et al. 2006.) The results if their study show that the flwo in the pharyngeal airway of OSA patients is comprised of a turbulent jet formed by are restriction in the velopharynx, which in turn leads to higher pressure in the velopharynx. Jeong et al. deduce, that the most collapsible are in the pharyngeal airway of OSA patients is the velopharynx where minimum intraluminal pressure and maximum aerodynamic force is situated. The study employs a CFD approach to asses plausible mechanisms of airway occlusion in OSA patients. Various fluid dynamic parameters, such as pressure drops, velocity distribution, wall shear stress, as well as the distribution of wall force caused by pressure at various locations inside the airway are calculated using various inspiratory flow rates. The reliability of the CFD model was based on assessment of performance of a low Reynolds number turbulence model in

predicting transitional turbulent flows. This was chosen as these transitional turbulent flows are the predominant flow characteristics in the pharyngeal airway. The CT images (or, more precisely, the segments of interest) were transformed to actual 3D models with the help of commercial Bionix Body Builder software (Ver 3.0, CANTIBio Inc., Suwon, Korea). A 3D triangular mesh was then generated by four iterations of Laplacian and boundary-edge smoothing algorithms. HyperMesh (Ver 5.0, Altrair Engineering, Troy, Minnesota) software was used to mesh the inside of the 3D surface with the tetrahedron element with the options of standard growth and normal mesh generation. It is reported to be necessary to create at least two cell layers next to the inner boundary of the 3D model to obtain a stable solution for tetrahedral meshes to employ the damping function. The quality and detail of the constructed model is quite high, especially taking into account that the study was performed in 2006. Airflow velocity was calculated at 9 different cross-sections. It is discussed that using CFD models, that only represent laminar of turbulent flow completely ignore the transitional nature of the actual airflow, which is ignored by basic CFD software. Complex flow phenomena may be reconstructed using more advanced turbulence models, such as Large Eddy Simulation (LES) and Direct Numerical Simulation (DNS). However, LES requires significant computational power, as the its accuracy is limited by the smallest grid size (this method is described in more detail in section 2.3 of this thesis). DNS is also claimed to be very expensive, as the grind density required for its use is proportional to Re^3. Thus the Jeong et al. chose a low Reynolds k-ε model instead, as the main features of laminar-transitional-turbulent airflows can be simulated using it. (Jeong et al. 2006.) Thus one other goal of the paper of Jeong et al. is also to validate the low Reynolds k-ε turbulence models, more particularly, the ability of its solution of transitional turbulent flow in a constricted tube. For this, experimental validation was performed comparing the results of a low Reynolds k-ε model with those of a standard k-ε model and experimental data.

Jeong et al. conclude, that the most important feature of flow in the pharyngeal airway of OSA patients is the turbulent jet that forms at velopharynx due to are restriction. It causes higher shear and pressure forces in the area of the velopharynx, thus the intensity of the mentioned turbulent jet may be the determining factor whether the pharyngeal airway collapses and causes larger deformation.

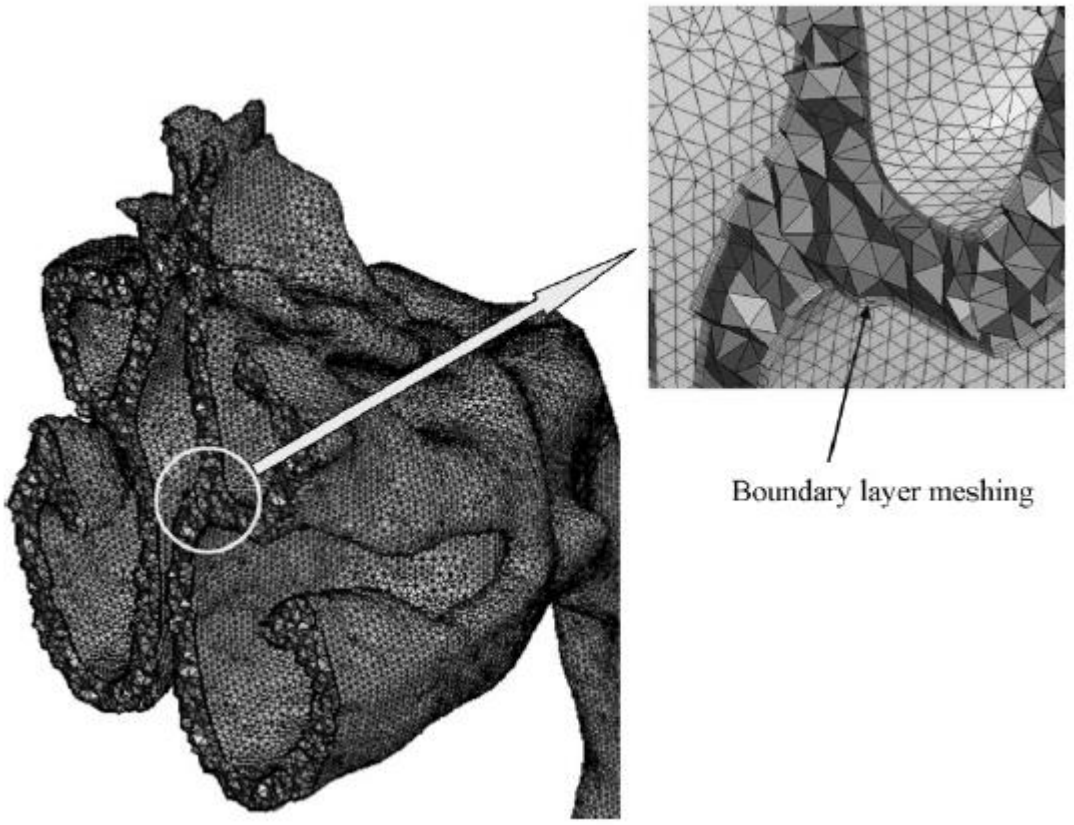

Figure 2.9. *The mesh obtained in the study Jeong et al.(Jeong et al. 2006)*

Wang and Elghobashi (Wang & Elghobashi 2013.) developed a direct numerical simulation solver with the lattice Boltzmann method (LBM), which they used to investigate the flow in upper airways of two patients. The patient-specific models were reconstructed from CT scans. Obstruction in the upper airway is located by using the time-averaged first spatial derivative of pressure (pressure gradient), $\delta p/\delta z$, while the second derivative, $\delta^2 p/\delta^2 z$, is used to exactly locate the obstruction. The study concludes that the solver which they used can be used to obtain accurate flow details in the upper airway and to locate the obstruction as well. (Wang & Elghobashi 2013.)

The objective of Wang and Elghobashi's study was to numerically investigate the flow in the upper airway, including the nasal cavity, pharynx, larynx and trachea) using DNS-LBM and to develop a method for location of the obstruction based on fluid dynamic properties of the flow. For this purpose, a DNS-LBM solver in 3D was developed on the standard LBM with stream-collision procedures. The solver was validated by performing several simulations of canonical flows. There were small discrepancies in the canonical flow simulations using this solver and other more common solvers, but overall the results agreed with analytical solutions and with experimental and numerical results. (Wang & Elghobashi 2013)

Upper airway models from 2 patients are considered, one from a healthy subject - the other of a patient with adenotonsillar hypertrophy (figure 2.10).

(a) Normal UA. Left: sagittal view; Right: dorsal view.

(b) Obstructed UA. Left: sagittal view; Right: dorsal view.

Figure 2.10. *The models used in Wang & Elghobashi studies (Wang & Elghobashi 2013)*

Wang and Elghobashi studied both inspiration and expiration flows. Recirculation flow, secondary flow and jet flow were found in the upper airway. The results showed that the amplitude and frequency of pressure fluctuations were reduced in the obstructed upper airway. A method for locating the obstruction in the upper airway was introduced, which is based, as already mentioned, on first and second derivatives of pressure, the former of which locates the region of the obstruction and the latter pinpoints the exact location of the obstruction. This method was validated by comparison to a normal upper airway that had two artificial obstructions. (Wang & Elghobashi 2013)

2.2. Finite element modelling

FEM was used in several studies as well. Some researchers have used 2D finite element modelling, but due to the complex geometry of the upper airway anatomy, it is a gross

estimation and does not accurately describe the actual phenomenon.(Xu et al. 2009; Huang et al. 2005) Xu et al. introduced a 3D finite element model using advanced MR tissue tracking, spatial modulation of magnetization (SPAMM) and reconstruction of a 3D structure from a stack of axial MR images (image-based modelling).(Xu et al. 2009)

In the 2009 study of Xu et al., MR images were taken to acquire the anatomy of the upper airway of a rat, including the soft tissues, and then one more series of images were taken during a controlled dynamic collapse of the upper airway, applying pressure using a tracheotomy. This data was used to model the event. The model was generated from a fast spin echo image set, using Amira® (TGS Template Graphics Software, Inc.). The required regions were divided using colour masking and made into a 3D representation. Images, acquired using pressure, which was applied through the tracheotomy, were used to produce different tissue regions (nasopharynx, oropharynx, tongue and other soft tissue) in the upper airway. Dynamic MR data was used to determine motionless tissue, such as the dorsal / posterior wall, skull, hard palate, mandible and others. Tongue, soft palate and lateral tissue were investigated. Triangular surface meshes were reproduces for all the different regions using HyperMesh from Altair. The meshes were converted to tetrahedral volume elements and imported to FE modelling software (ABAQUS/CAE 6.4, HKS Inc. Pawtucket, RI). SPAMM was used to determine coupling of different anatomic regions. Negative intraluminal airway pressure was used as a model boundary condition on the tissue bounded by nasopharynx and oropharynx. Rigid regions were fixed, tissue boundaries that have notable motion were modeled as traction-free surfaces. Soft tissue was modelled to have linear elastic properties. Contact pairs automatically specified the contact and sliding between the dorsal tongue and ventral palate surfaces as the airway collapsed. Constraints were applied where there was no motion. Rostral and caudal tongue ends were allowed motion in the ventral-dorsal and medial-lateral directions. The model in two positions can be seen in figure 2.11.

The 3D FE model of Xu et al. (2009) simulates motion and displacement direction of important tissue groups and collapse of oropharynx and nasopharynx. The results of the model showed similar tissue displacements and airway deformation when compared to dynamic MR image data. It was found that the model, in which heterogeneous pharyngeal tissues were used showed better relation with the dynamic MR study, comparing with the model, which modelled all the tissues as uniform. This shows that pharyngeal tissues have a different Young's modulus and that it should be taken into account when modelling the upper airway. (Xu et al. 2009)

However, as the study used a rat to model the upper airway, it was consequently simplified, as a rat's upper airway anatomy is less complex than that of a human. It was chosen because one can simulate an airway collapse in a rat at one's convenience, while in humans sleep has to be either induced or occur naturally and only then can dynamic sleep MRI be performed, which in itself is rather complex due to the fact that the patient tends to move involuntarily during sleep. In addition, the amount of tissue types and orientation was simplified to incorporate the ones that could be tested directly.

Furthermore, the tissues were described as linearly elastic, which is a gross simplification for biological tissues and actual non-linear data should be used to describe the mechanical properties of the tissues. The model only used static air pressure, thus the effects of airflow were not included in it. In addition, FE model has its own limitations in regions where tissue displacement is very small.

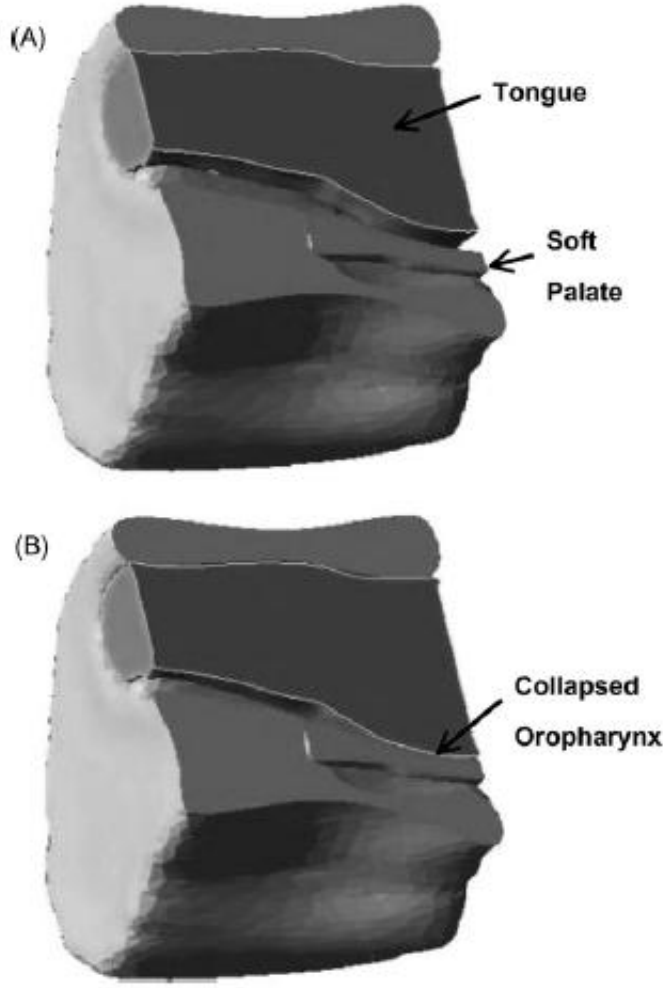

Figure 2.11. *The FEM model of Xu et al., showing the collapse of oropharynx in B and the normal situation in A. (Xu et al. 2009.)*

Huang et al. in another study also employs FEM to model the upper airway from MRI data from 5 patients. As seen in figure 2.12, the model also includes the genioglossus muscle and other structures. The model is described as a "pressure-/state-dependent model of genioglossal muscle contraction under laminar flow conditions". (Huang & Malhotra et al. 2005.) It was developed based on skeletal muscle microstructure and the cross-bridge theory. Direct relationship between the signals measured with EMG (electromyography) and the actual muscle fibre contractions are shown. This model was then incorporated into a 2D computational model and FEM was used to simulate airflow. It is concluded in the study that using this method the EMG signals can be directly incorporated into the model, thus avoiding the measurement of

the speed of muscle contraction, which is complex. In this way, structural anatomical data (for instance, from MR imaging), EMG, or muscle activation information and tissue mechanical properties can be incorporated into a computational model and help produce a detailed analysis of upper airway collapsibility.

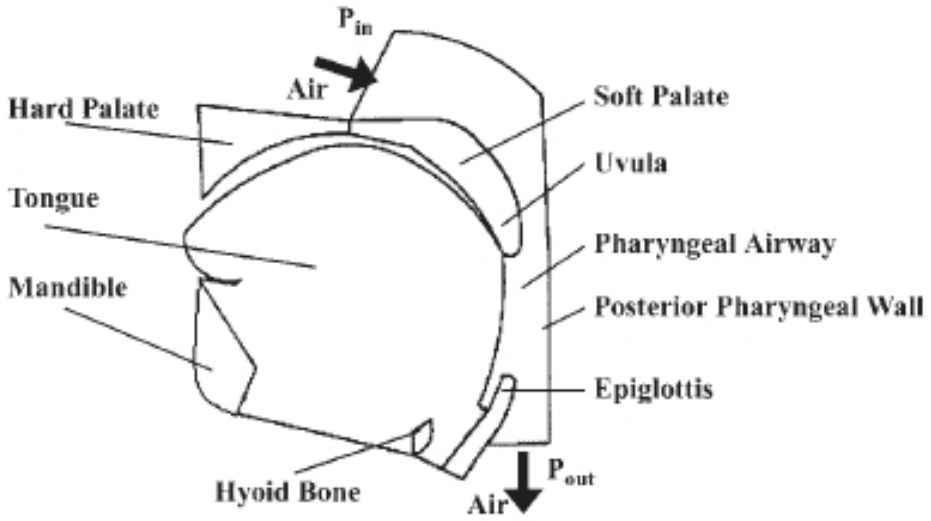

Figure 2.12. *Model derived from MRI images in the study of Huang & Malhotra et al. (Huang & Malhotra et al. 2005.)*

Huang et al. in another study use the FE model described above and MRI data from 5 patients to construct 2D models of upper airway that simulate upper airway collapse. Only tongue muscle is included in the model. The model was used to simulate the upper airway collapse after mandibular advancement, palatal restriction and palatal stiffening procedures. EMG data for the contraction model was obtained from published results. As there was no data for the same patients during sleep, it was estimated instead based on literature, that the genioglossal muscle is approximately 15 per cent less active.

Below in figure 2.13 the results of this study can be clearly seen. It shows that the normal pharyngeal airway collapses at -13 cm H_2O pressure, and after mandibular advancement it drops to -21 cm H_2O, after palatal restriction to -18 cm H_2O and after palatal stiffening to -17 cm H_2O. (Huang & Malhorta et al. 2005.) Thus mandibular advancement can be said to be the most effective treatment according to this study.

However, 2D modelling is inherently less informative than its 3D counterpart, thus some information is inevitably lost and overlooked. The biggest advantage of this model is claimed to be the connection of EMG data with the contractile force. This means that, according to this study, EMG data can be directly incorporated into the model, and complex measurements, such as muscle shortening velocity, as needed in modelling the behaviour of the muscle, can be avoided. The final model requires input of MR image data, muscle behaviour data from EMG and mechanical properties of tissues to produce a detailed finite element analysis of collapsibility of the upper airway. It is claimed further, that the model is very applicable and that it can mimic the behaviour of the genioglossus muscle adequately. In addition, when and if more experimental data on

muscles associated with the upper airway is available, the model could be amended, according to Huang et al. Based on the data of isometric muscle experiments available at the time of the study, it is concluded that the predicted muscle behaviour is similar to that of the experiments at hand. The model also predicts, that at the waking time the muscle is about isometric, due to the fact that the length of the activated genioglossal muscle fibre is maintained in a negative pressure range.

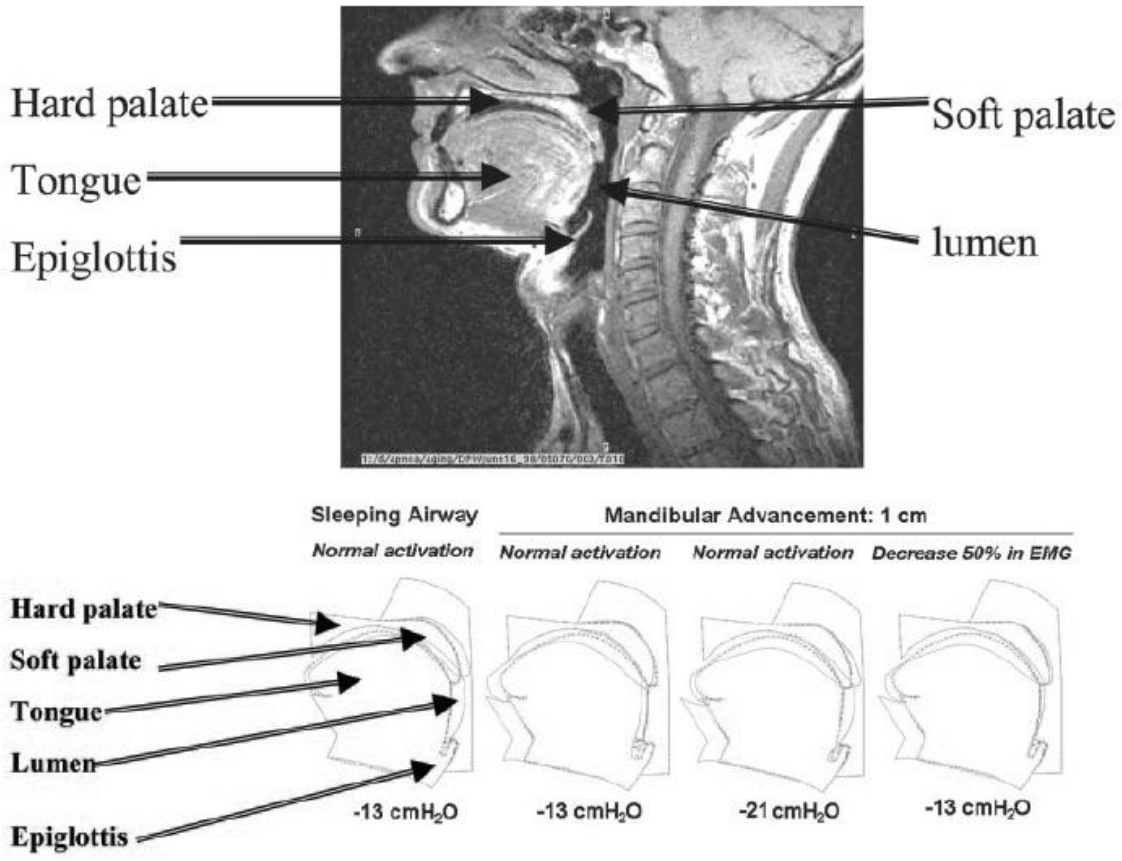

Figure 2.13. *Results of the study of Huang et al. (Huang & White et al. 2005.)*

2.3. Large Eddy Simulation

LES is characterized by division of the flow field into large and small scales by a filtering procedure. While in the RANS (Reynolds-Averaged Navier-Stokes) method averaged results are provided by modelling all the turbulent scales, LES directly solves the equations that describe the evolution of large turbulent scales. Only the smallest scales are modelled by using Sub-Grid-Scale models. It also allegedly can provide an increased level of detail and accuracy for unsteady, separated and vertical turbulent flows. (Mihaescu et al. 2008.)

LES is claimed to be a more accurate approach than the common RANS (Reynolds-Averaged Navier-Stokes) method. It considers a flow model reconstructed from cross-sectional MRI images. The airway model is characterized by the maximum narrowing site at the retropalatal pharynx. Three approaches were used nonetheless: RANS with

two steady turbulence models and the unsteady LES, using commercial computational fluid mechanics software Fluent®. In RANS, both *k-ε* and *k-ω* turbulence models are used. The model in the study was reconstructed from MR images. (Mihaescu et al. 2008.) Figure 2.14 shows the results of simulations using these 3 methods.

In the 2008 study of Mihaescu et al., MR images from one OSA patient were acquired. It is reported, that the boundaries (needed for extraction of the upper airway from the acquired MR images) were determined using an Edge Detection Programme (EDP). These boundaries were then inputted to a mesh generator called Gambit (Fluent®) as Cartesian coordinates. Then the computational model was generated. As results, the largest differences were found in axial velocity distributions downwards from the maximum narrowing of the upper airway.

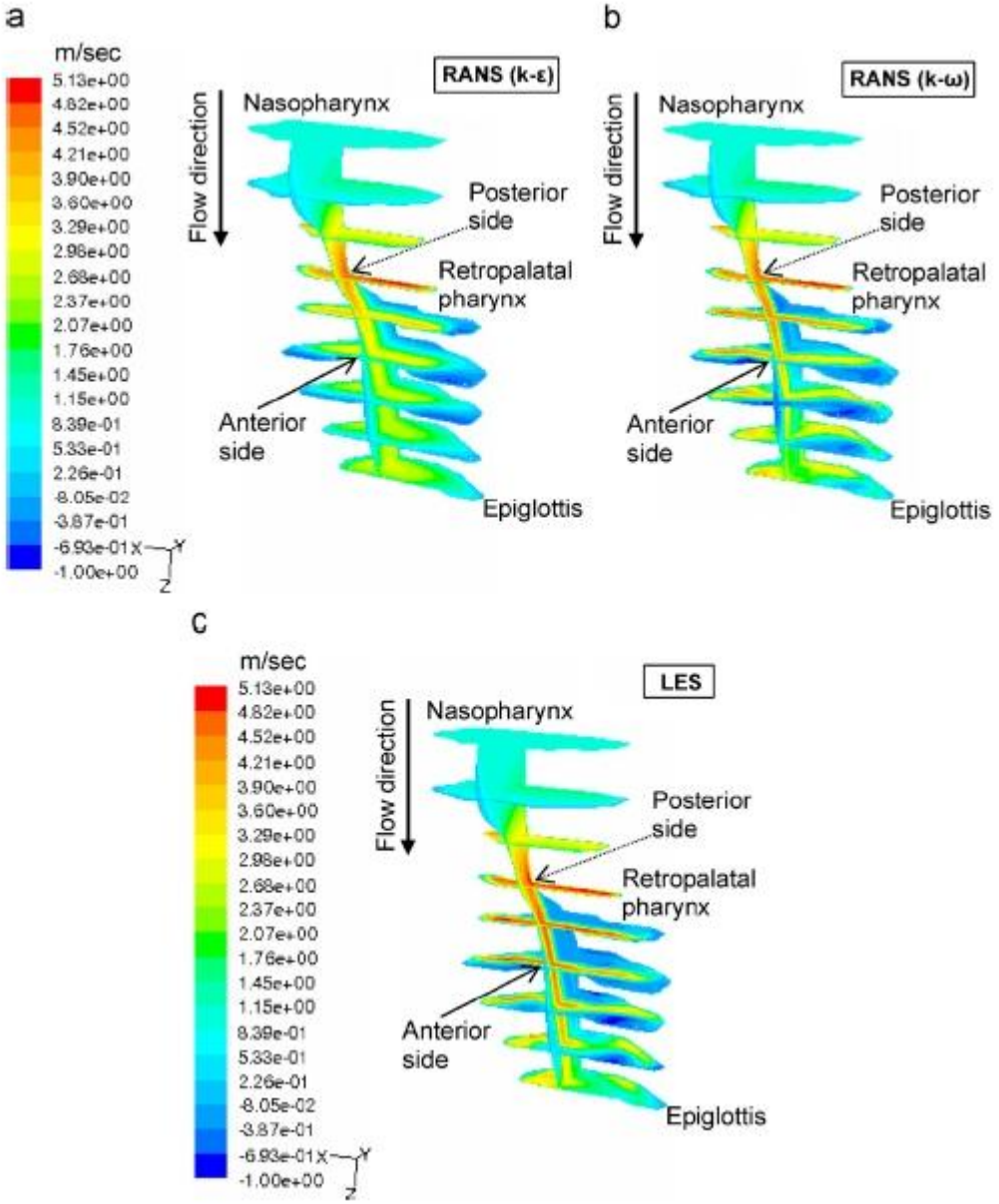

Figure 2.14. *Results from Mihaescu et al. simulations: velocity distributions in different axial planes (Mihaescu et al. 2008.)*

In a further LES study, CT imaging data and CFD were employed to describe the flow behaviour in the pharyngeal airway of a patient with OSA. Cone beam CT was used to capture the images needed, while the patient was lying in a supine (flat on the back) position. Upper airway scanning was performed with 0.4mm slice thickness. Pre- and post-surgery models were reconstructed from cross-sectional CT data using medical imaging software Mimics® (Materialise, Belgium). The LES option is selected from within the CFD software package Fluent 6.2 (ANSYS®, USA), for capturing pharyngeal airflow dynamics associated with the OSAS subject at pre- and post-treatment. (Mihaescu et al. 2011.) This was validated with the same model as in the study of Mylavarapu et al., 2009.

2.4. Other studies

Chouly et al. numerically predict and experimentally describe the flow induced deformation in a simplified tongue, in interaction with an expiratory airflow. An in vitro model is proposed, using which measurement of deformation of the artificial tongue can be done. Asymmetries in geometry and tissue properties are accounted for in the experimental model (the two major physiological characteristics of the upper airway). The numerical method for prediction of the fluid-structure interaction uses the theory of linear elasticity in small deformations to compute the mechanical behaviour of the tongue. The boundary layer theory is used to describe the main features of the flow. The numerical method predicts tongue movement with error of 20%. It was also described, that while entering an obstruction, the air is accelerated, due to constant flow rate. After passing the constriction, the flow decelerates and tends to form a wall-bounded jet (figure 2.15).

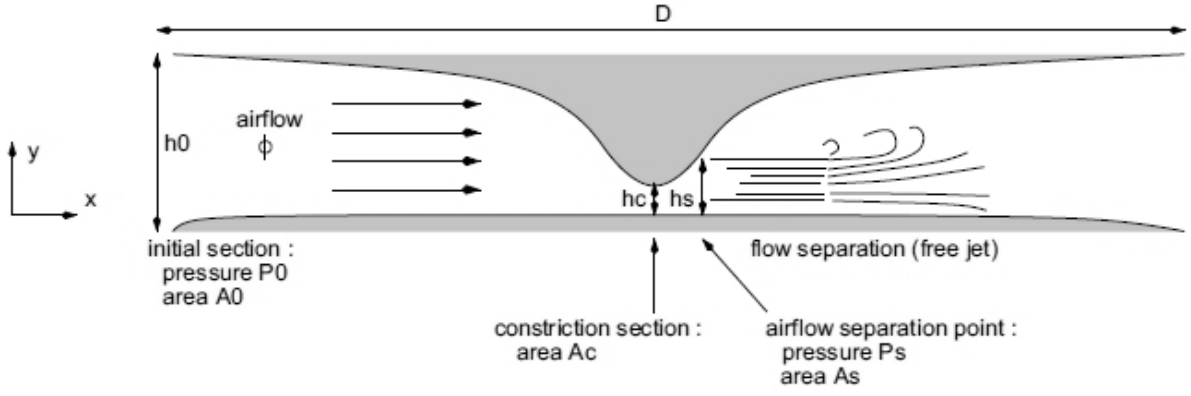

Figure 2.15. *Airflow through a constriction. (Chouly et al. 2008.)*

Huang et al. investigate sleep apnea from the mechanical point of view using a model, which is claimed to be realistic and includes surrounding structures: the skull, the neck, the hyoid bone, cartilages and soft tissue. The respiration process was simulated with the fluid-structure interaction method (FSI) and with computational fluid

dynamics (CFD). Rigid wall conditions were used in the CFD method. CT image data was used for finite element modelling and was first processed with Mimics® 10.0 software (Materialise, Belgium). Then some geometric irregularities were corrected and a 3D model made with inverse CAD software (Geomagic Studio 10.0, USA). The FSI method proved to be more feasible and effective than CFD. As CT images were used as a source of data in this study, it was easy to include some cartilage and bone structures associated with the upper airway, namely 4 of them were included: epiglottis, thyroid, cricoid and tracheal cartilages. However, as CT does not provide good information on muscles, none of them were included in the model, even though they play a very important role in the upper airway system. (Huang et al. 2013.)

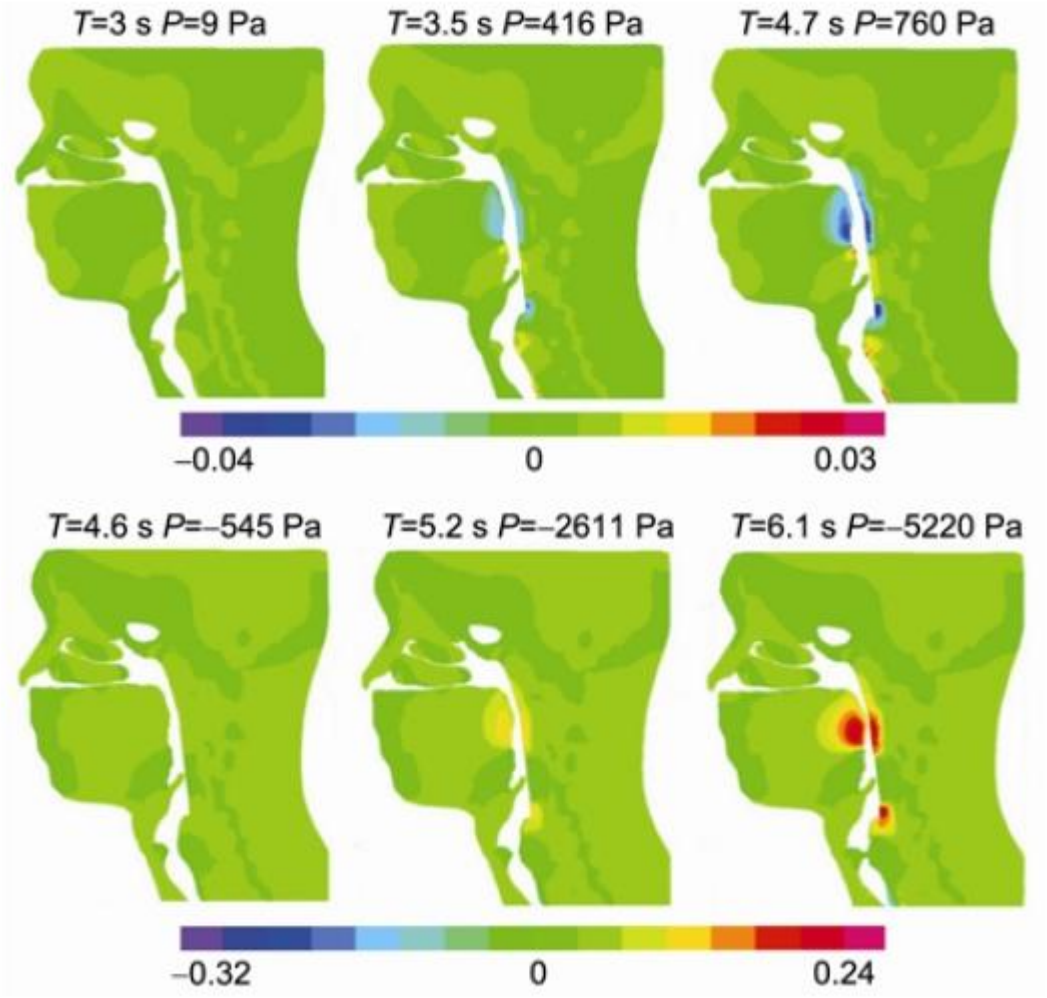

Figure 2.16. *Results of Huang et al. simulation of airflow during a sleep apnea episode (Huang et al. 2013.)*

Aittokallio & Gyllenberg et al. (1999) present a mathematical model of the upper airway of an OSA patient, which predicts the nasal flow profile from three critical points that control the upper airway patency during sleep. Nasal pressure prongs were used to determine kinetics during airflow collapse. The model includes the respiratory pump drive, the stiffness of the pharyngeal soft tissues and the dynamic support of the

muscles surrounding the upper airway. The model reproduces the airflow of the OSA patient depending on these three components.

Farré et al. investigate airflow using an analogue model, called the Starling model for a collapsible conduit (figure 2.17). The Starling resistor consists of an elastic fluid-filled collapsible tube mounted inside a chamber filled with air. The static pressure inside the chamber is used to control the collapsibility of the tube. This model allows interpreting the mechanics of the upper airway using two parameters: critical pressure P_{crit} and upstream resistance R_{up}, which both can be measured using non-invasive techniques and thus can be used to assess upper airway mechanics during sleep non-invasively.

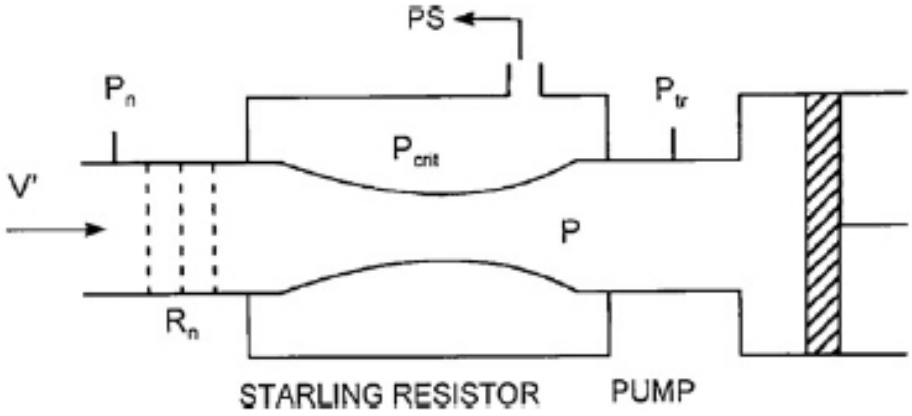

Figure 2.17. *Respiratory model based on a Starling resistor for the collapsible upper airway used in the study of Farré et al. (Farré et al. 2008.)*

Donelly (Donelly 2010) describes the use of MR imaging for surgical planning for persistent sleep apnea patients. It concludes that the combination of information about anatomic abnormalities and patterns of collapse can help in surgical decision making. Both of these subjects can be described using sleep MRI studies, which include sequences that evaluate both static anatomic as well as dynamic motion of the airway, which is crucial in proper diagnosis of sleep apnea. It was said that in most cases sleep MRI even changes the surgical management decisions. (Donnelly 2010) It was also statistically shown that there is a greater chance of OSA decreasing when the surgical decisions are based on sleep MRI than when they are not. In the institution where Donnelly's study was performed patients are referred for MRI sleep studies when they are already diagnosed with OSA by other means, usually polysomnography. In addition, indications include persistent OSA despite previous surgery (most often tonsillectomy and adenoidectomy) and anticipated complex airway surgery for OSA, among others. It is also reported that children with Down syndrome are common OSA patients, as they are predisposed with increased propensity for adenoid tonsil regrowth, increased propensity for adenoid tonsil regrowth, increased propensity for lingual tonsil enlargement, glossoptosis and hypopharyngeal collapse. The most common identified entities include recurrent enlargement of the adenoid tonsils, enlargement of the lingual

tonsils, abnormal soft palate, glossoptosis and hypopharyngeal collapse. Figure 2.18 below shows images acquired from a sleep MRI study showing a hypopharyngeal collapse event in sagittal and axial fast gradient echo cine images.

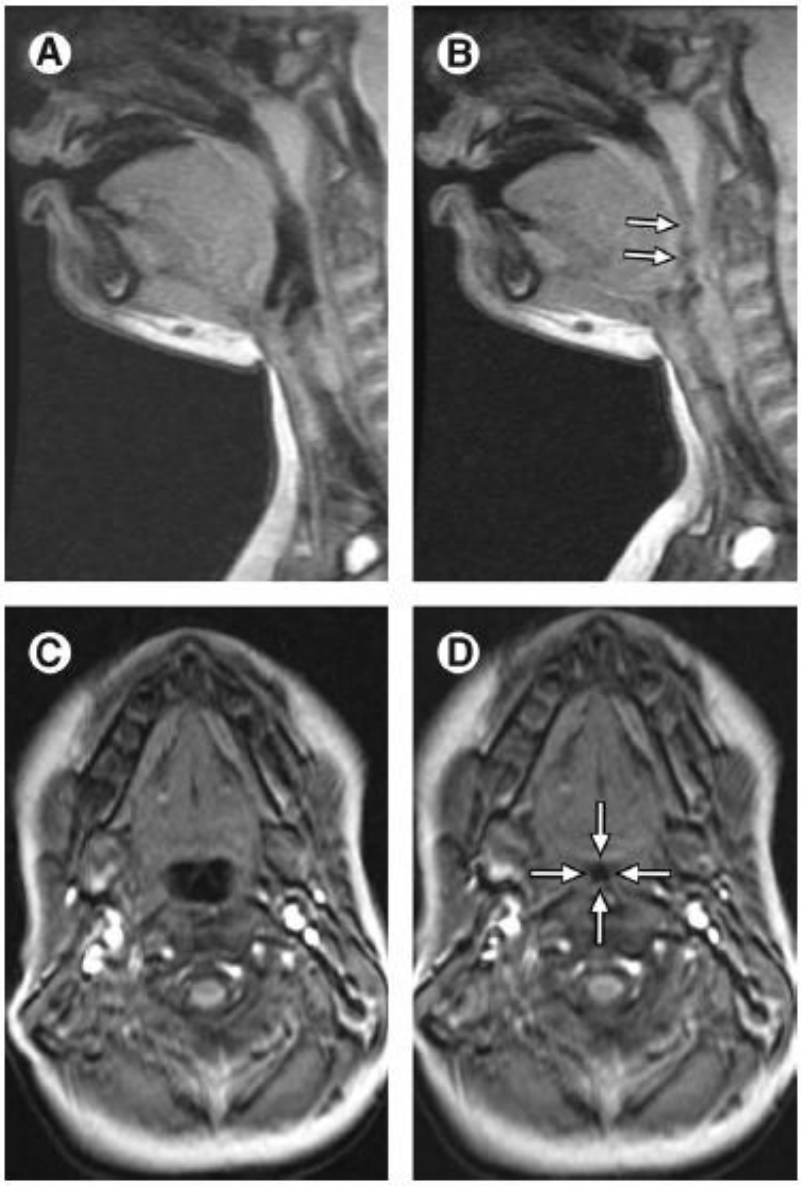

Figure 2.18. *Sleep MRI study MR images, showing hypopharyngeal collapse in sagittal and axial planes. A - sagittal image at expiration shows retroglossal airway to be patent; B - Sagittal image at inspiration shows collapse of the retroglossal airways; C, D - events of A and B, respectively, in the axial plane (Donnelly 2010)*

Most of the above-described studies used some way, completely mechanical or computational, to introduce the dynamic element, i.e. the airflow to the static model. Static analysis of MR images, that is segmentation of separate relevant anatomical groups (the airway, surrounding muscles and bones) will be discussed from a practical point of view in the next chapter.

The study of Zhu et al. (Zhu et al. 2012) deals with the movement of the soft palate during calm respiration. Soft palate, as it is one of the soft tissue structures associated with the upper airway may contribute to airway collapse. Thus the movement of it was studied. To this end MR image sequences of a healthy male subject were used and a model of the subject was reconstructed. As seen in figure 2.19, the model includes the nasal cavity, nasopharynx and oropharynx.

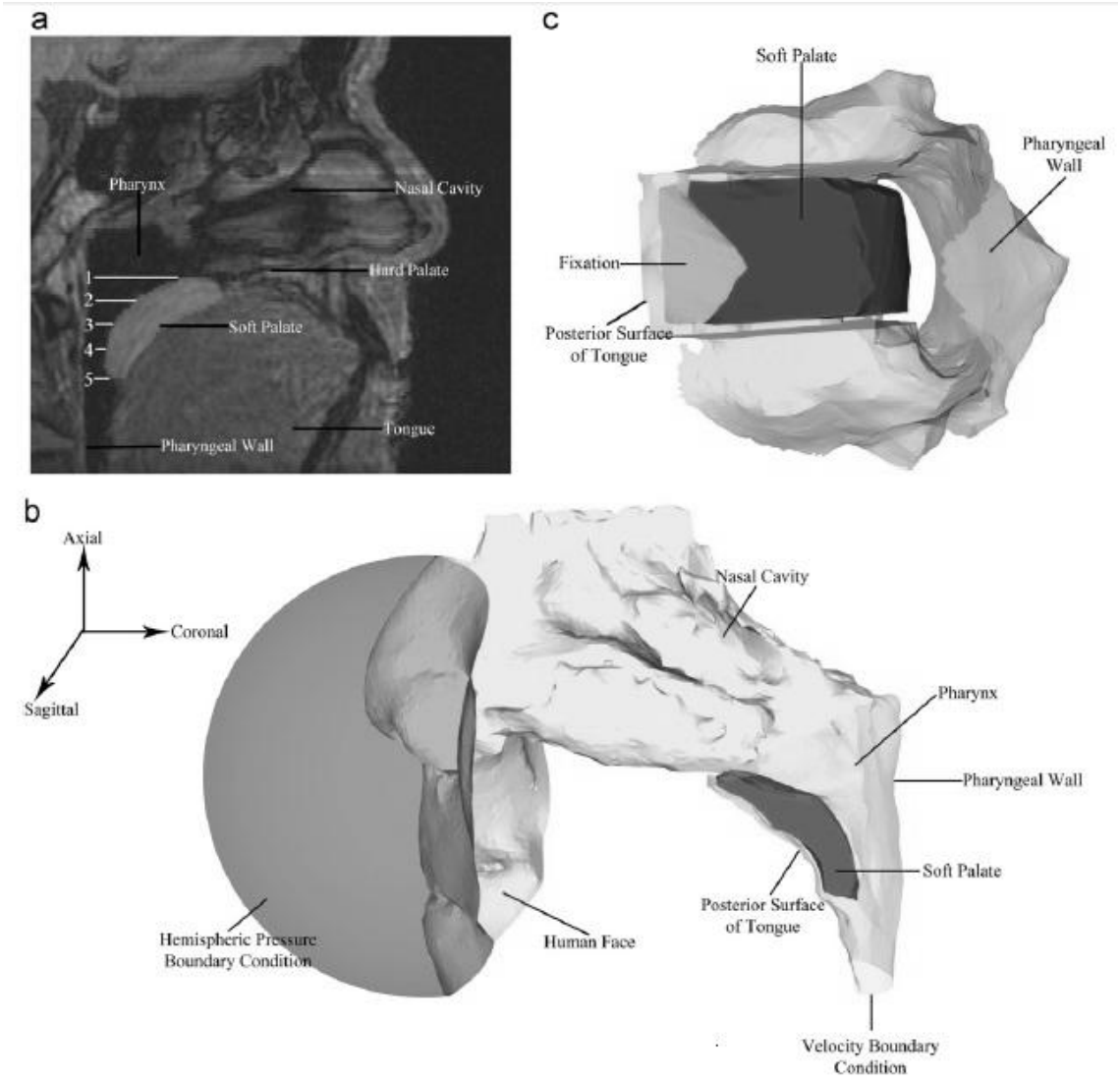

Figure 2.19. *Segmentation and modelling configuration in the study of Zhu et al. a - sagittal image of the upper airway with soft palate marked, b - the fluid model, c - the structural model. (Zhu et al. 2006)*

The study makes some assumptions, such as that the airflow in the upper airway is laminar (which as described in the sections above is not exactly the case) and that the soft palate is linearly elastic (which is also not the case with most biological tissues). The ventilation rate in the simulation was 7,5 L/min. Simulations were carried out for two respiration cycles, with soft palatal Young's modulus set as 7539 Pa. The soft palate was almost static during inspiration but moved towards the posterior pharyngeal wall

during expiration, Zhu et al. report. Thus, it is also reported, that this movement of the soft palate during expiration might well contribute to the airway collapse.

The further sections of this thesis take a more practical stand. Firstly, the materials and methods used in this thesis are described in detail, concentrating mostly on the segmentation task, but also including a description of the literature review in brief. It is followed by presentation of results, which mainly are rather graphic in this thesis. Discussion of various issues that arose during the work on this thesis comes afterwards. There, there is a detailed description of the difficulties and shortcomings as well as the significance of what has been done in this thesis. Finally, some conclusions and the list of references are presented.

3. Methods and materials

Acquisition of the static upper airway model is vital in the process of upper airway modelling. Thus, the following chapter of this thesis deals with segmentation of MRI image sequences from 3 patients, that were taken prior to and after orthognathic surgery. The process of acquiring a static model of the upper airway system includes analysis of imaging data of the upper airway and surrounding tissues, usually MRI or CT imaging data. Then, with the help of segmentation software, the structures of interest are extracted from the original data using segmentation. The goal of segmentation in this thesis is not only to see the effects that orthognathic surgery has on the upper airway system, as the name of thesis itself would suggest, but also to aid the creation of an upper airway model. MRI is used as it provides a more detailed view of soft tissues and muscles than CT, and they play a very important role in the mechanism of obstructive sleep apnea, thus it is prudent to include them in the static model.

It is to be said that the literature review, described in detail in the previous section of this thesis, was performed using scientific databases, for which Tampere University of Technology provides access. The most widely used databases were *PubMed*, *ScienceDirect* and *IEEE xplore*. It can be said that a fair amount of papers (including the most recent ones) were reviewed for this thesis, as the abovementioned databases provide a vastly wide array of papers of interest, even if the topic of modelling of airflow during sleep apnea generated not that vast an amount of related papers. Furthermore, some papers were added to the review after the initial review, which took place in July-August of 2013 (some papers were added in 2014 as well), mainly because the topic of upper airway modelling is gathering more and more attention and more papers are continuing to be published all the time.

As for the practical side of this thesis, MR images from 3 patients (pre- and post-operative sequences) have been used in this thesis as the data source. The images were acquired with a 3 tesla Siemens® Trio™ MRI scanner (Siemens Medical Solutions, Erlangen, Germany). Each imaging sequence is a t2 weighted 3D imaging sequence. Echo time (Te) was 407 ms and repetition time (Tr) was 3200 ms. One slice is 0.9 mm,

voxel - 0.9 mm^3. Each sequence contains 512 slices, the resolution of the images is 512x512 pixels. The images were acquired in Tampere University Hospital, Department of Radiology in various dates from 2010 through 2013 (this is because it takes a long time from initial orthognathic surgery planning to actual surgery). The described sequences were provided in DICOM format.

The segmentation was performed semi-automatically and manually using ITK-Snap (Ver. 2.4.0, Yushkevich, P.A. et al.) open source software, which has been validated clinically (Yushkevich et al. 2006.) The ITK-Snap software has a user-friendly interface, and is a highly specialized segmentation tool, meaning the features of it are concentrated on the segmentation task, which include different semi-automatic segmentation routines, manual segmentation tools, post-processing tools and also 3D image navigation tools. While many other software tools (for example the aforementioned ImageJ, a popular tool Slicer 3D), especially open-source ones, are over-packed with different features and thus require significant time to learn to use them according to one's needs, one can start using ITK-Snap almost immediately, even if one does not possess significant mathematical or engineering skills. The main user-interface window consists of 4 smaller windows, in which the image series in question are placed in axial, sagittal and coronal slices with one window displaying the segmented 3D model of the segmentation in process. The original image slices are connected in such a way that one can select one point in one of the slices, say, the axial slice, and the same point will automatically be selected in other two views, thus making it easy to navigate through the images and analyze structures of interest.

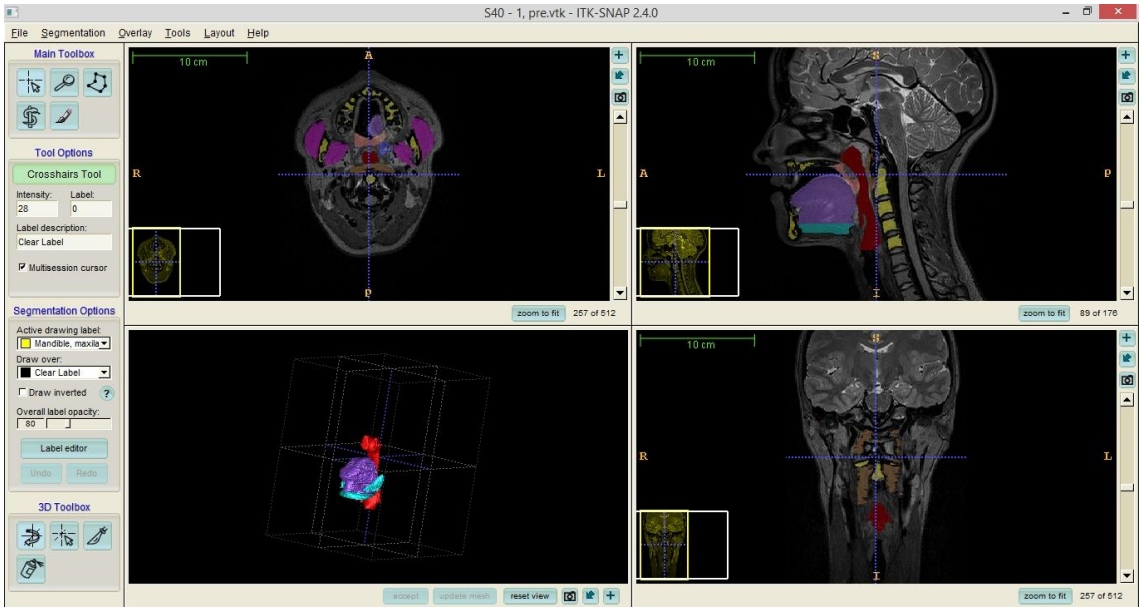

Figure 3.1. *The main window in ITK-Snap, showing three slices of the MR images with some segmentation and the segmentation 3D model, also presented in the results section*

As already mentioned, there are both manual and automatic tracing options. Labelled regions are represented using an integer-valued 3D mask image of the same dimensions as the input image. Each voxel can be assigned a label or left without a label. Region definition in the case of manual tracing would be done with a brush tool. If a voxel has already been assigned with a label, it can be made so that one cannot override it while another label is being assigned to a structure next to the said voxel. The automatic, or rather semi-automatic tracing includes two tools, one based on different gray values and the other based on edges of different structures in the image. Both include the initial addition of seed points, or "bubbles", as they are called in the software, which then proceed to expand according to the setting chosen beforehand. These are different gray values in the former tool and different edges in the latter. Thus the outcome of the semi-automatic segmentation depends upon the mentioned tools, specifically the way, in which the images are converted into a probability map or speed function, the initial contour and the values assigned to different factors that drive the contour evolution. All these rather cumbersome tasks can be performed with ease using the segmentation wizard in the software.

The process using the wizard consists of three stages. The first stage is for choosing the method from two 3D active contour segmentation methods: Geodesic Active Contours and Region Competition. (Yushkevich et al. 2006.) Both methods use one or more contours are used to estimate the structure of interest. Probability maps are computed by applying a smooth threshold, which is two-sided or one-sided, depending on where in the histogram the structure of interest lies. The effect of filters applied to the selected slice can immediately be seen in other two slices, for inspection. In the second stage the segmentation is started by placing bubble or bubbles in the image for active contour growth. The last stage is for specifying the weights of the various terms in the active contour evolution.

The software is capable of opening various typical medical imaging files, including DICOM standard files, which were used in this work. The segmentation itself is saved in a VTK file.

The 3D models were smoothened using built-in Gaussian smoothing and another, unspecified, 3D smoothening option.

The structures, that were segmented for each image sequence, are: upper airway, temporomandibular joints, lingual tonsils, mandible, maxilla, 4 top vertebrae (in the case of patient 3 - 3), genioglossus muscle, mylohyoid and hyloglossus muscles, inner and outer masseter muscles, soft palate and stylo-pharyngeus muscle. The muscles were selected because they are the biggest and most significant, the jaws were included to see how they were altered, the vertebrae - to see if they are shifted, and other structures because they are in the proximity of the jaws and are susceptible to being shifted somehow. In addition, temporomandibular joints were included because at times they might be shifted during orthognathic surgery and it is actually important that they remain in the same position, for the proper function of the jaws. However, in the end it was decided, that the main results are to be the segmented upper airway combined with

the genioglossus, mylohyoid and hyloglossus muscles, which includes less information, that was initially planned to include, but nonetheless is informative, and such models were not published before (at least to the best knowledge of the author of this thesis based on the literature reviewed).

4. Results

As one of the most important tasks to be carried out in this thesis was the segmentation of the upper airway system, the results of segmentation of the MRI image sequences are presented in this section. They are presented as follows: for each of the 3 patients there are two figures, each having two series of images. One of the series (the top one) is the pre-operative series, while the lower one is the post-operative series. The first figure of a patient shows original MR images (just a few slices, as there are 512 slices for each position) for the reader to get a better view and understanding of the second figure, which, in turn, shows the segmented 3D structures of the upper airway and genioglossus, mylohyoid and hyloglossus muscles. Each figure has 6 images, marked with letters A, B and C. The image marked A and the image below it are both images in the sagittal plane. The image marked B and the image below are in the axial plane, and the last, C images, are in the coronal plane.

In addition, the figures of the segmented images also contain some volumetric data, namely, the volumes of the upper airway, genioglossus muscle and mylohyoid and hyloglossus muscles. The volumes are presented as pre- and post-operative values. Appendix 1 contains tables of all of the above and additional volumes of segmented structures, as initially more values and more structures were planned to be added to the figures.

The results also show figures of additional segmented structures, such as additional muscles, soft tissue structures and skeletal structures, even though the most important figures are the ones that begin the results.

After the presented images an interpretation of some of the results is presented, with further discourse being postponed until the discussion section. This part of the page is left blank intentionally so that the result pictures could be grouped as two per page to provide a clearer view for the reader, as the logical place of result interpretation is after the figures.

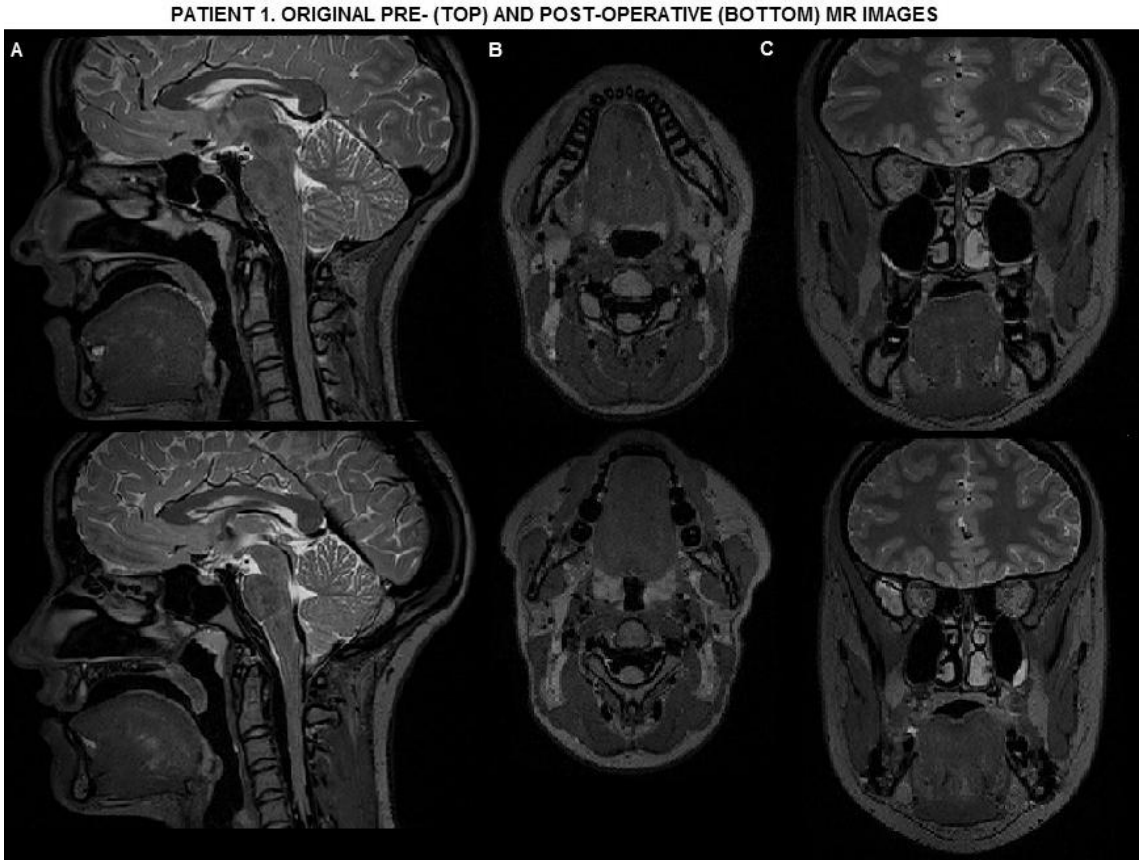

Figure 4.1. *Original MR images of patient 1. A - sagittal view; B - axial view; C - coronal view.*

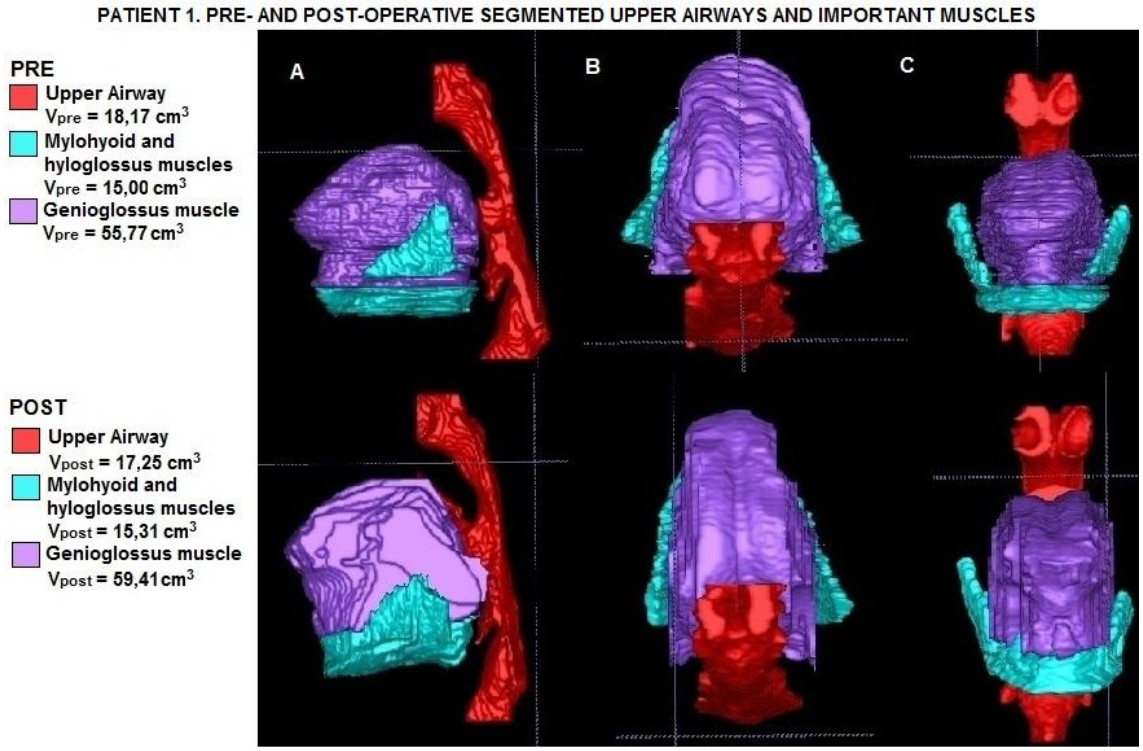

Figure 4.2. *Airways and muscles segmented from MR images of patient 1. A - sagittal view; B - axial view; C - coronal view.*

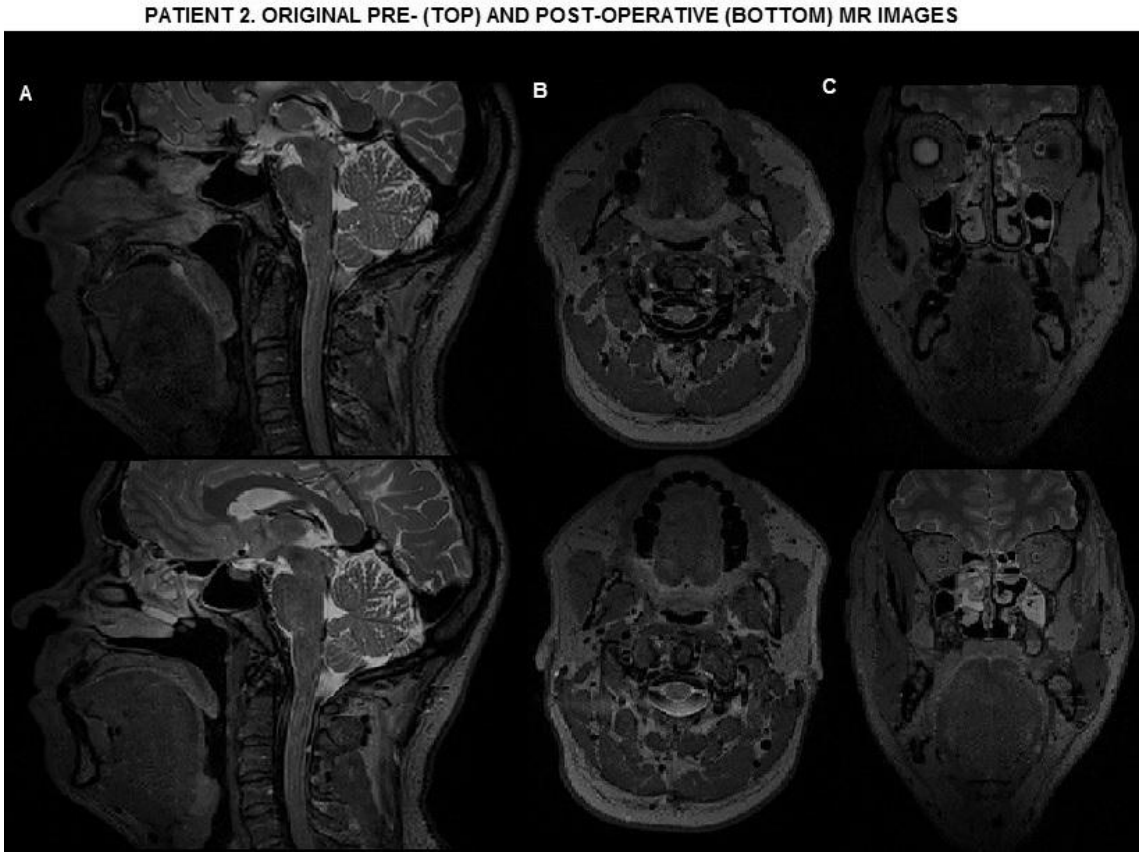

Figure 4.3. *Original MR images of patient 2. A - sagittal view; B - axial view; C - coronal view.*

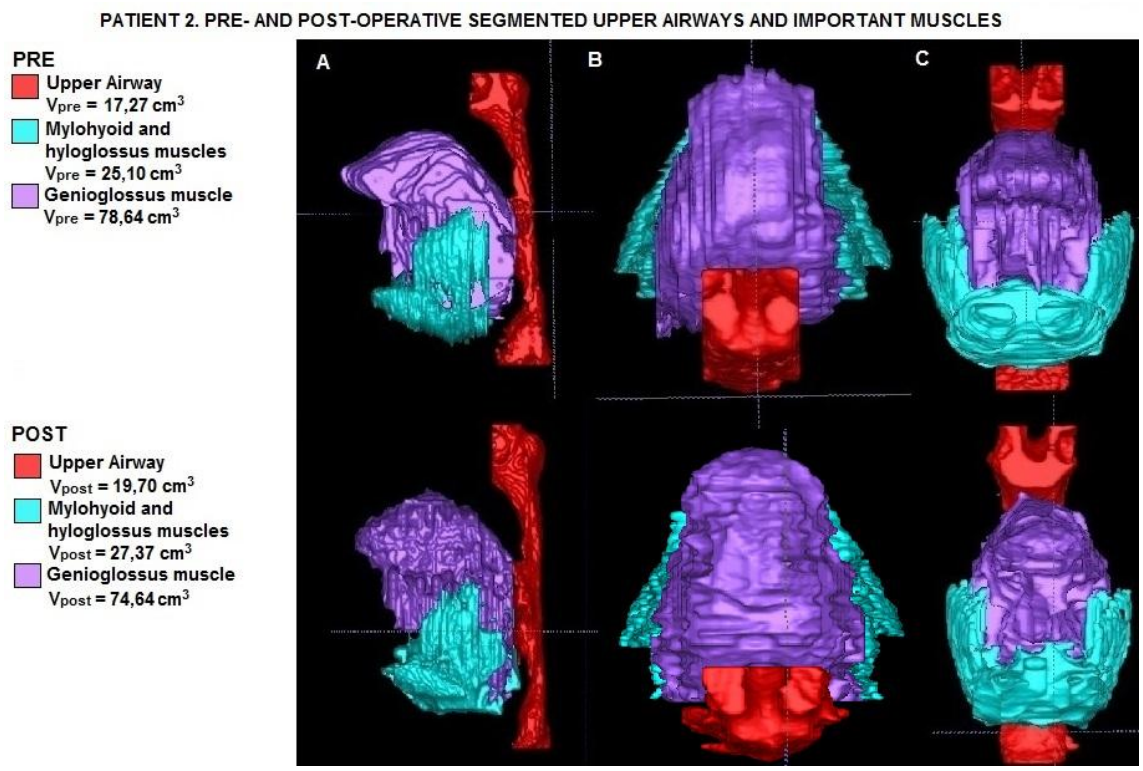

Figure 4.4. *Airways and muscles segmented from MR images of patient 2. A - sagittal view; B - axial view; C - coronal view.*

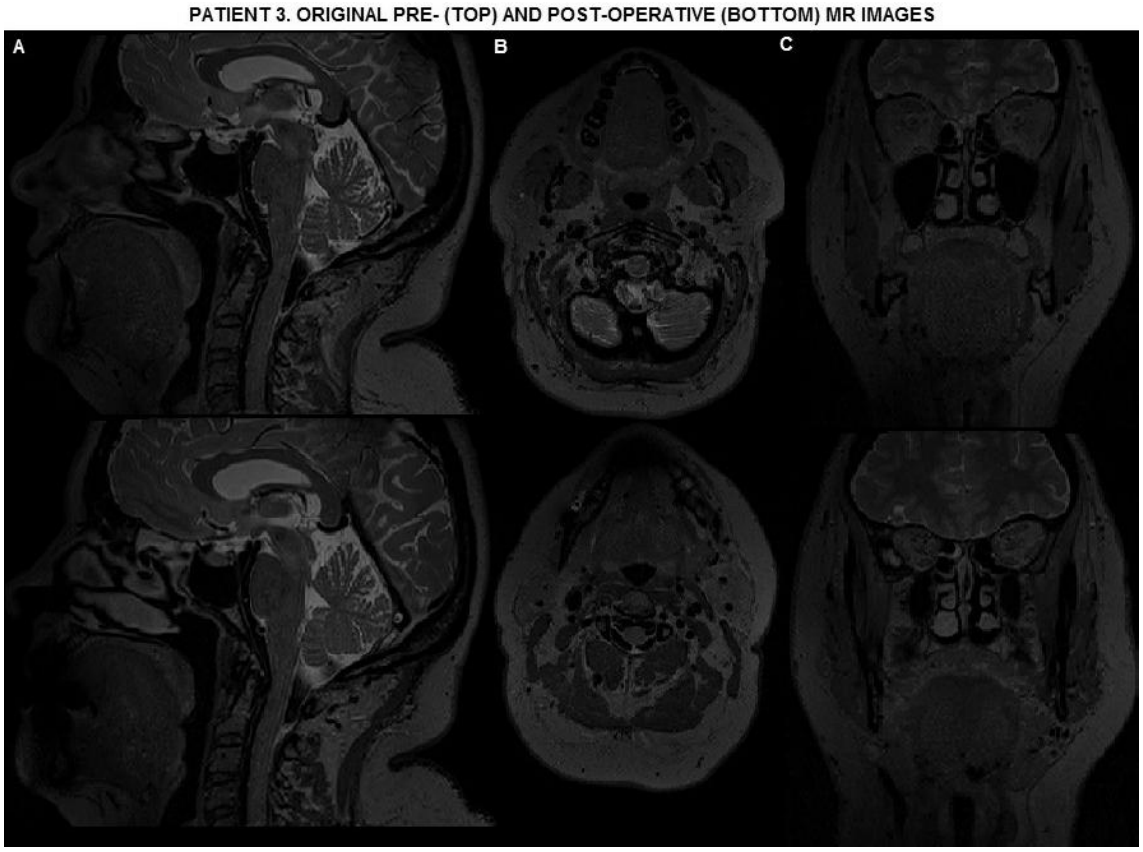

Figure 4.5. *Original MR images of patient 3. A - sagittal view; B - axial view; C - coronal view.*

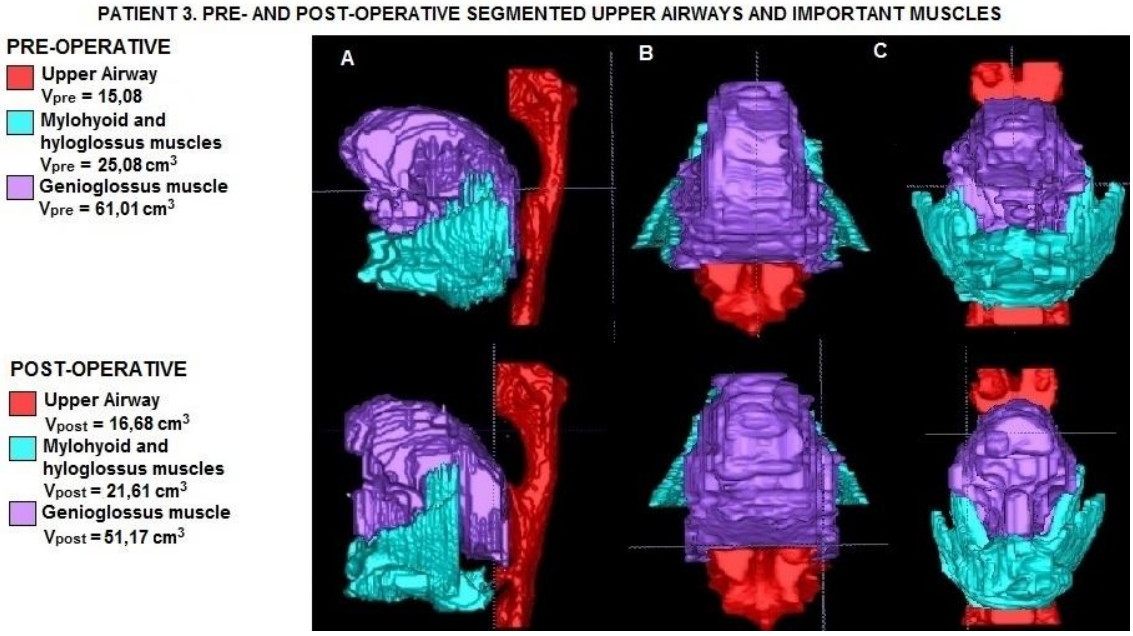

Figure 4.6. *Airways and muscles segmented from MR images of patient 3. A - sagittal view; B - axial view; C - coronal view.*

For patient 1 it can be clearly seen in the axial (B) view, that after surgery the genioglossus muscle has become elongated, comparing to the pre-operative situation.

On the contrary, for patient 2 the genioglossus muscle seems to be widened after the orthognathic surgery. The genioglossus muscle of patient 3 seems to widened too.

The most significant increase in the volume of the upper airway is observed for patient 2 (with the increase of). Upper airway of patient 3 also increased, by . Interestingly, the airway of patient 1 seems to have shrunk.

In general, there are morphologic changes in the muscles that are tied to the jaws. Also, the upper airway seems to be wider in all three cases, even if the volumetric data indicates a slight decrease in volume in patient 1.

The tables showing volumes of the segmented structures as automatically calculated in the ITK-Snap software are presented in Appendix 1. Red colour in the difference column indicates, that the difference in volume of the structures prior to and after the operation is negative, i.e. the volume decreased. Then green colour in the difference column indicates, that the difference in volume of the structures prior to and after the operation is positive, meaning that the volume increased.

It can be observed, that the general tendency is for the volume to increase, however, not in all cases. The upper airway of patient 1 actually decreased in volume, even though it appears to be wider.

Lingual tonsils increased in volume in all three cases, according to the data. However, the change recorded was minute, and should not be regarded as a serious change in the structure of the tonsils.

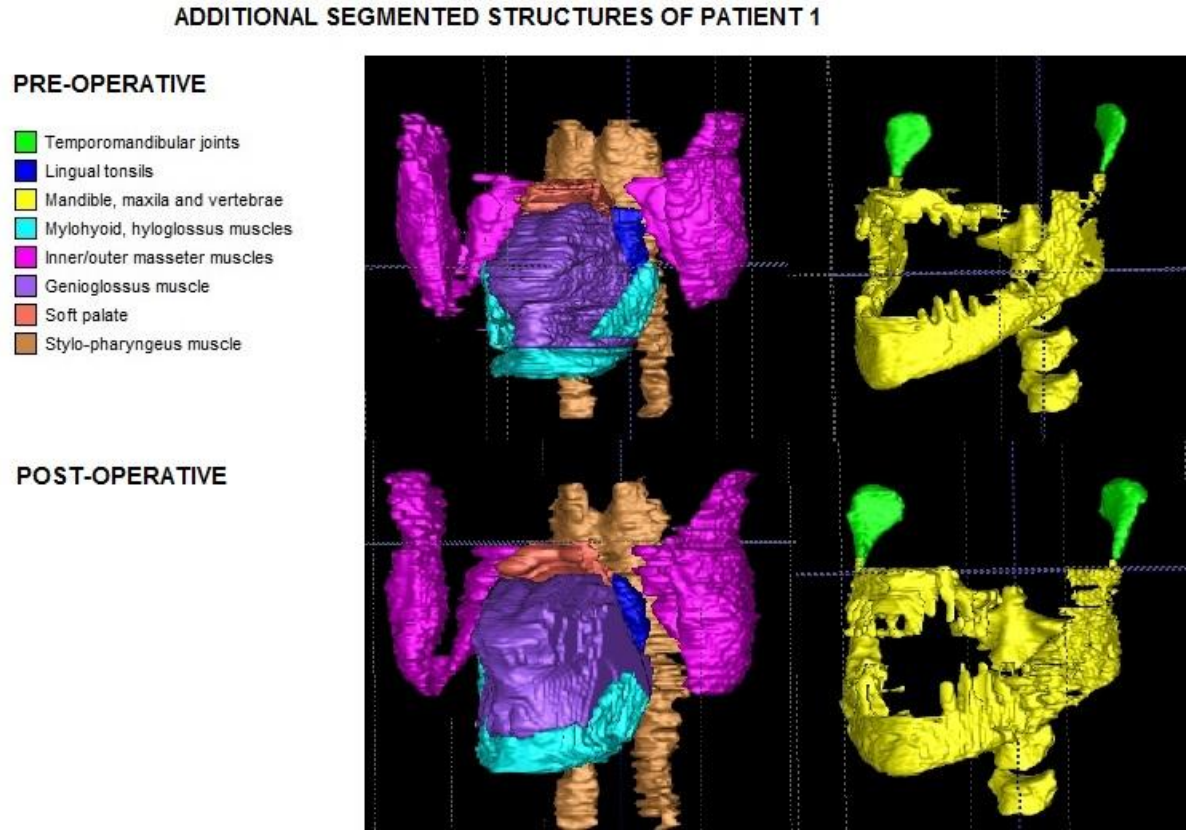

Figure 4.7. *All segmented muscles, soft tissue structures and skeletal structures for patient 1, from the pre-operative image sequence.*

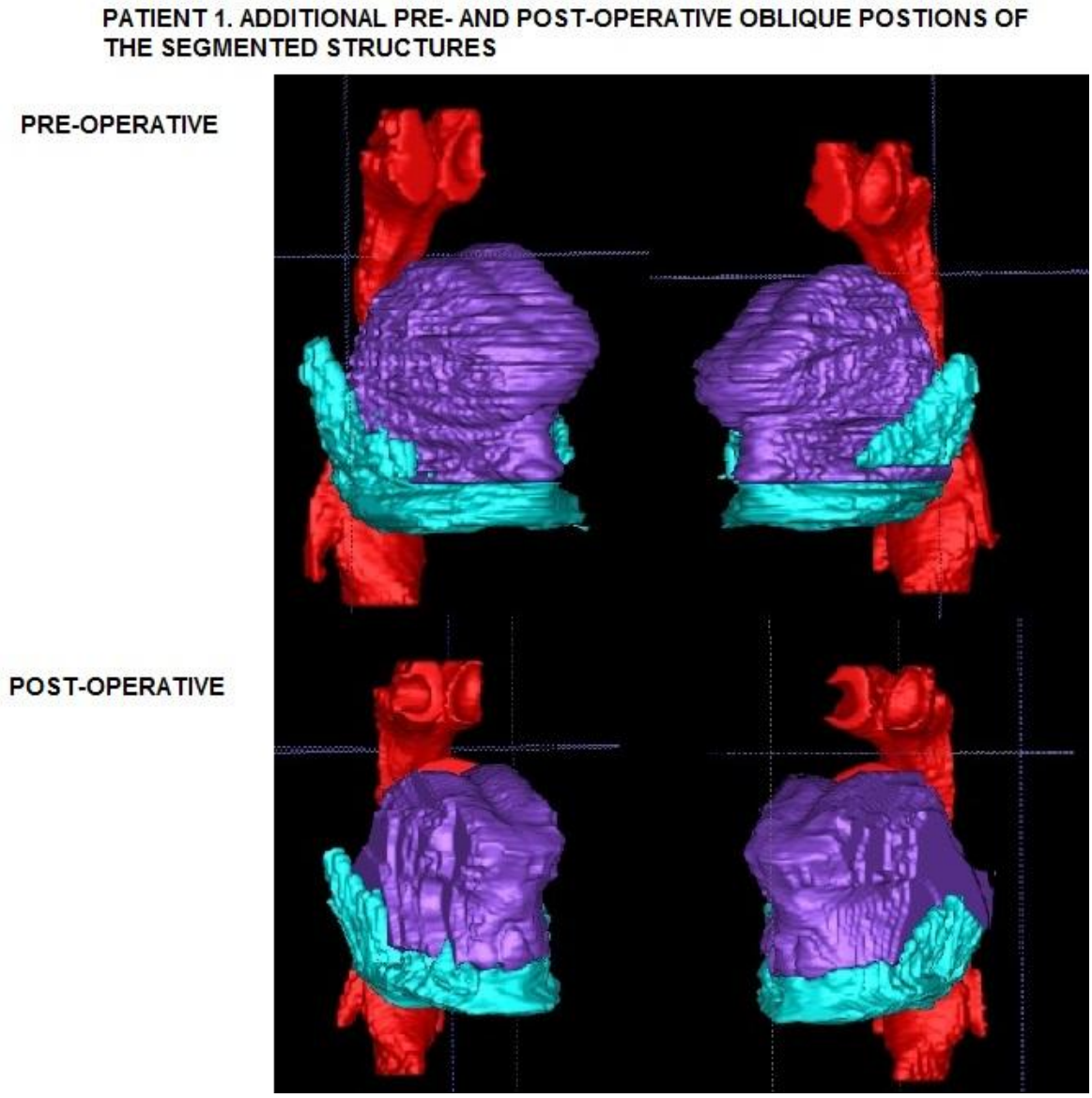

Figure 4.8. *Additional oblique positions of structures presented in figure 4.2.*

As it was also attempted to segment other structures, not only the ones presented in figures 4.2, 4.4 and 4.6, they are presented above, in figures 4.7 and 4.8, figure 4.8 added for comparison of all the structures prior to and after the operation.. The structures presented in figure 4.7 are from patient 1, pre-operative and post-operative image sequences, respectively. The most obvious effect of the surgery (indeed the intended effect) is that the maxilla and mandible are now in a normal position, in contrast to the situation in the top of figure 4.7, where clearly the mandible is protruding to the front (a condition called mandibular prognathism).

In addition to figure 4.7, one more figure is presented, 4.8, showing oblique positions of the structures presented in figure 4.2.

5. Discussion

As of 06.02.2014, there were no publications, that included muscles, segmented from MR image sets of human patients into the 3D models used in simulation of airflow in the upper airway. There was, however, a 2D model (Huang et al. 2005) and a 3D FE model of the airway of a rat, than did include the tongue muscle. Nevertheless, researchers tend to concentrate only on the upper airway itself without adding other structures to the model. This may be due to the fact that it is quite complicated to include the required properties of the muscles (such as contraction speeds and so forth) to the model when they are included. That might be overcome by using EMG recording of the muscle activity, as described by Huang et al. (Huang et al. 2005). The segmentation in this paper did produce muscles in addition to the upper airway itself, not only the tongue muscle, but it was later decided to include only the tongue muscles in the final model.

The literature review made it clear that computational fluid dynamics is the most used and researched way of introducing the dynamic element (airflow in this case) to the static upper airway model. There was, however, no consistency in what specific muscles and structures were included in the model, this seems to be a preference of the researchers. However, it is to be said, that as manipulating the jaws also affects the tied muscles and the airway itself, it is an inter-related system, and at least the biggest muscles (such as the genioglossus, superior pharyngeal constrictor and stylo-pharyngeus) should be included in the static model.

The results (specifically the volumetric data) are not consistent throughout the 3 patients. This might be due to many reasons. The first and foremost reason is the segmentation itself. As the differences are not that significant and the segmentation process was also partially manual, it is best to avoid drawing any drastic conclusions from the volumetric data. It was indeed hard to distinguish between the structure being segmented and the surrounding tissue at times, especially in the case of less homogenous structures, such as the muscles segmented, but also the maxilla. In addition, the morphology of the muscles changed after surgery, thus making it even harder at times to determine, where the muscle ends and where it begins.

There is no consistency in the change of muscle volume. Mylohyoid and hyloglossus muscles increased in volume in first two patients, but decreased in the third. Inner and outer masseter muscles decreased in volume in patients 1 and 3, but increased in patient 2. The genioglossus muscle increased in volume in patient 1, but decreased in patients 2 and 3. The change in muscle volume has to be attributed to error, because they should not change, as the performed surgery only manipulated the jaws, not the muscles themselves. Thus mostly the error is due to manual segmentation, which had to be used considerably a lot, as will be described in the further text. If one would be to take the volumes presented in the figures 4.2, 4.4 and 4.6 in the results section of this thesis and choose the most differing muscle volumes (except those of patient 3

genioglossus muscles, as the MR image sequence itself was corrupt in the post-operative sequence exactly in the posterior of the tongue, as can be seen in bottom image A in figure 4.5), one would find that those are the genioglossus muscles of patient 2, and the error from that can be derived as 5%. However, that might not reflect the reality totally, thus a more realistic error would be 10%, because the error cannot be derived only from the volumetric analysis.

Initially it was planned so that ImageJ would be used, but due to the fact that while ITK-Snap provides a very user friendly interface with only the essentials of segmentation, ImageJ has numerous complex extensions. However, as ITK-Snap was run on a computer that had Windows 8 64-bit operating system, there were numerous unexpected glitches and strange behaviour of the software in general, which delayed the work. These included sudden crashes, non-responsiveness, visual glitches, such as failure to show some certain windows and settings. In addition, quite a lot of segmentation had to be either done manually entirely or had to be corrected manually. This was because it was at times really difficult to distinguish between different muscles and surrounding tissue just by looking, let alone by semi-automatic segmentation. In general, only the upper airways themselves and temporamandibular joints could be properly semi-automatically segmented.

It has to be mentioned, too, that the segmentation performed was not automatic, and semi-automatic only in a certain sense. The "snake" tool, which was chiefly used in the ITK-Snap software provides two options of extracting the required structures, namely image intensity region filtering (one of the 2 automatic tracing options, based on different gray levels in the image) and image edge filtering. The former tool is considerably more useful and convenient, even though it is far from perfect in less homogenous structures, such as the genioglossus and other muscles. The image intensity filter allows one to set a boundary gray value level, to make structures above or below a certain grey level stand out from the image. It can also be used as a notch filter, meaning that both above and below values can be used at the same time. However, even at the more homogenous structures, such as the soft palate, the grey level might vary quite significantly (one of the causes of this is noise in the images), and thus it is near impossible to track the structures very accurately, except in the case of the upper airway itself and the temporomandibular joints, which could be tracked with almost no difficulties (comparing to other structures especially). The snake tool itself works in such a way that one adds a bubble (or bubbles, as one sees fit) in the structure, and it "grows" from there. As the edges of most of the structures are not so clear, it considerably more often than not went over the edges, and that had to be corrected for manually using the manual tracing tools for every of the 512 slices, which increased the time required to segment the images significantly.

The image analysis, i.e. the segmentation of MR images in this thesis used static MR images of healthy (in this case meaning non-sleep apnea) patients as a source. For a more specific, detailed and more-to-the-point analysis dynamic sleep MRI studies should (and will, according to the author's knowledge) be made additionally. This is

because sleep apnea only occurs during sleep, and the specific upper airway movement, also the movement of associated important structures (not only muscles, such as genioglossus, but also for example the soft palate and the uvula) can only be accurately analyzed from sleep MRI data. This would also automatically validate the model being constructed, thus there would be no need of, for example, mechanical models, which were built in many of the reviewed studies to validate the computational models.

Figure 4.7 in the results section shows all the other structures, which were segmented from the provided MR image sequences. It shows these structures as segmented from the pre-operative sequence of patient 1. One can observe, that the quality of skeletal structures that were segmented is rather poor. This segmentation was attempted to see, if it is plausible in any way that MR imaging could replace CT imaging completely. With the current quality of MR images, it takes a rather long time to extract the skeletal structures from them. Given that the MRI quality increases considerably in future, it is plausible that it could completely replace CT imaging, at least in the maxilofacial are imaging.

Segmentation of non-homogenous structures with unclear boundaries, such as, for example the genioglossus muscle and the muscles below it, namely mylohyoid and hyloglossus, is rather error prone and complex. If this is to be done for every patient in orthognathic surgery planning, some way needs to be found to automate the process, possibly with the use of algorithms, but even then it is highly likely that the final segmentation would need to be corrected manually. Cheng et al. in their 2009 paper state that the geometry extraction and manipulation process are the most time-consuming and labour-intensive parts, because of low resolution CT data sets compared to the actual complexity of the human nasal cavity structure. In the case of MRI the situation is the same, paradoxically, due to greater detail and resolution of the images. Even so, the quality of MR imaging still needs to be improved, if it is to fully replace CT, especially CBCT, which is popular in the maxillofacial imaging. Namely the number of slices per each scan should be increased, thus decreasing the size of the voxels and pixels that form the image. In addition, noise should be considered very carefully and in the best case scenario avoided as thoroughly as possible. This is because it can produce falls results, especially as usually the person, who is segmenting the images is not a professional of medical sciences.

The main results produced are presented in figures 4.2, 4.4 and 4.6. However, additional results are presented as well. Figure 4.7 shows all the pre- and post-operative segmented structures that were segmented. Additionally, figure 4.8 shows two more positions of the segmented structures presented in figure 4.2, which were at first suggested to be put in the final figures, but were not included, due to the fact that the traditional 3 orthogonal projections (sagittal, axial and coronal) sufficient anatomical information. Figures 4.8 is perhaps more visual to non-medical professionals and may in effect provide an additional view to the reader.

In addition, it has to be mentioned that it is important that the position of the head of the patient during the pre- and post-operative imaging sessions be in the same position,

normally in the supine position. This is because the airway geometry depends on the position of the head in the way that the upper airway is more collapsible when the head is in the supine position, as structures, such as the soft palate, the uvula and even the genioglossus muscle are more prone to blocking the airway, especially if the airway is already pathologically narrowed or just inherently narrow. The slice thickness in the CT data sets in the study of Cheng et al. varies from 1,25 mm to 3 mm, most being 2,5 mm thick. That is not adequate for acquisition of detailed meshes of the upper airway. However, even though the slices of MRI data sets used in this thesis were 0,9 mm thick it was still not adequate for convenient and not too labour-intensive extraction of the nasal airways.

If this work was to be continued, nasal airways should be included in the model, as it is an important part of the upper airways. It was not included in the current model due to the disproportional workload and an inherent lack of quality in the MR images. Thus, the model provided by this thesis is not complete. Despite this, many publications presented models, which do not include the nasal airways as well so it would still be applicable to actual airflow simulation modelling. Furthermore, the obstructions responsible for obstructive sleep apnea are situated in the part of the upper airway before the nasopharynx, thus it is sufficient as it is. However, it would still be strongly advisable to include the nasal airways for authenticity of the airflow that can be achieved via modelling, even though that could be simulated without the inclusion of the nasal geometry.

Before application of the segmentation results to actual modelling, the VTK files should be exported into a mesh software and transformed into a mesh, while also smoothing it further. The mesh can be produced using ITK-Snap software, but the smoothing that the software provides is insufficient.

In addition, it would perhaps be more relevant to acquire the static models of the upper airways from actual sleep apnea patients, for the reviewed scientific articles as a rule employ both MR (or CT) image sequences of healthy subject or subjects and those of a sleep apnea patient. (Cheng et al. 2013; Zhao et al. 2013; Xu et al. 2006; Iwasaki et al. 2011; Wang et al. 2009; Jeong et al. 2007; Ito et al. 2011; Mylavarapu & Shanmugam et al. 2009; Mylavarapu & Mihaescu et al. 2009; De Backer et al. 2007; Sung et al. 2006; Persak et al. 2011; Sarasen et al. 2012; Mihaescu et al. 2008 and others.) However, as this thesis included analysis of images of both pre- and post-operative sequences and as there were some morphological changes in the upper airway geometries, it could still be relevant. For future studies, however, it would be advisable to include sleep apnea patients to the study.

One more thing to consider is the noisiness of source MR images. Especially significant was noise in the post-operative sequence of patient 3, where the front of the genioglossus muscle was missing. Less significant noise was found throughout the images, and may well have contributed to the error in segmentation, thus consequently also in the volume estimation of segmented structures.

6. Conclusions

A literature review of relevant publications was performed in this thesis, with some of the most interesting and significant studies described in more detail. In addition, a static 3D model of the upper airway system, including some of the muscles, most importantly, the tongue muscles, was constructed.

Based on the literature review performed in this thesis, it would be recommendable that computational fluid dynamics be used as the means of simulating the airflow in the upper airway model, with the further method of direct numerical simulation (DNS) or large eddy simulation (LES), which seem to be the ones that are most able to simulate the complex and specific airflow in the upper airways, including its collapse, where special flow properties are present. The model itself should include at least the genioglossus muscle, which plays an important role in sleep apnea, especially obstructive sleep apnea. The required parameters for muscle movement in modelling can be acquired using EMG, which was described in detail in Huang et al. 2005, and thus avoiding the need of complex muscle velocity measurements.

Drawing conclusions only from the volumetric data would not be advisable. Visual inspection of the segmented images can also provide significant information. However, the method used in this thesis is very time-demanding, and could hardly be implemented in clinical practice successfully. It could be done perhaps with less noisy and higher quality MRI images (which especially with patient 3 was a bit of a problem in this work), because the ITK-Snap software itself is quite versatile and also it seems to be developed constantly, as a new version has been just recently released. However, the volumetric data of the upper airway itself (not considering the nasopharynx due to high complexity of its anatomy and the inherent lack of imaging quality) can be rather easily obtained and analysed. It is to be said that as the patients, MR imaging data of whom was analysed in this thesis, were not sleep apnea patients, radical changes in the volume of the upper airway were not observed (the airway of patient 1 even decreased in volume).

ITK-Snap is a handy and convenient tool when it comes to segmenting homogenous structures with clear boundaries in 3D. However, it still needs considerable improvement for use with less homogenous structures, such as muscles, which has been done in this thesis and took a significant amount of time, as many tasks such as post-segmentation correction, as described in the whole document, needed to be done manually.

The static model acquired in this thesis can be applied for use in modelling despite its shortcomings, which have been discussed in detail throughout the thesis, especially in the discussion section.

As one of the questions raised before the thesis was that of the ability of MR imaging to fully replace CT in the future, it is concluded for now in the thesis that with current quality of MR imaging, the skeletal system cannot be adequately visualized only

with the help of MR imaging, thus the replacement of CT can only happen with significant increase of MR quality, as discussed in the thesis repeatedly, and perhaps with application of routines specially designed for skeletal system imaging using MR.

References

Aittokallio, T., Gyllenberg, M. & Polo, O. 2001. A Model of a Snorer's Upper Airway. Mathematical Biosciences 170. pp. 79-90.

Aittokallio, T., Virkki, A. & Polo, O. 2009. Understanding Sleep-Disordered Breathing Through Mathematical Modeling. Sleep Medicine Reviews 13. pp. 333-343.

Azarbarzin, A. & Moussavi, Z. 2013. Snoring Sounds Variability as a Signature of Obstructive Sleep Apnea. Medical Engineering & Physics 35. pp. 479-485.

Barrabé, P., Buisson, H.R., Tamisier, R., Levy, P. & Guméry, P.Y. 2002. Analysis of the Collapsibility of the Upper Airway in a Spectrum of Sleep-Disordered Breathing: A Modelling Approach. C. R. Biologies 325. pp. 465-471.

Bill, J., Proff, P., Bayerlein, T., Blens, T., Gedrange, T. & Reuther, J. 2006. Orthognathic surgery in cleft patients. Jurnal of Cranio-Maxillofacial Surgery, vol. 34, supplement S2. pp. 77-81.

Cheng, G.C., Koomullil, R.P., Ito, Y., Shih, A.M., Sittitavornwong, S. & Waite, P.D. 2013. Assessment of Surgical Effects on Patients with Obstructive Sleep Apnea Syndrome Using Computational Fluid Dynamics Simulations. Mathematics and Computers in Simulation. 16p.

Cheng, M., Phaneuf, C. & Tovar, B. Sleep Apnea Simulation: An Experimental Assessment of Pharyngeal Collapse. Department of Mechanical Engineering, The Cooper Union for the Advancement of Science and Art. New York. 12p.

Chouly, F., Van Hirtum, A.V., Lagree, P.-Y., Pelorson, X. & Payan, Y. 2008. Numerical and Experimental Study of Expiratory Flow in the Case of Major Upper Airway Obstructions with Fluid-Structure Interaction. Journal of Fluids and Structures 24. pp. 250-269.

De Backer, J.W., Vanderverken, O.M., Vos, W.G., Devolder, A., Verhulst, S.L., Verbaecken, J.A., Parizel, P.M., Braem, M.J., Van de Heyning, P.H. & De Backer, W.A. 2007. Functional Imaging Using Computational Fluid Dynamics to Predict Treatment Success of Mandibular Advancement Devices in Sleep-Disordered Breathing. Journal of Biomechanics 40. pp. 3708-3714.

De Backer, J.W., Vos, W.G., Verhulst, S.L. & De Backer, W. 2008. Novel Imaging Techniques Using Computer Methods for Evaluation of the Upper Airway in Patients

with Sleep-Disordered Breathing: A Comprehensive Review. Sleep Medicine Reviews 12. pp. 437-447.

Donelly, L.F. 2010. Magnetic Resonance Sleep Studies in the Evaluation of Children With Obstructive Sleep Apnea. Semin Ultrasound CT MRI 31. pp. 107-115.

Eckert, D.J., Malhorta, A. & Jordan, A.S. 2009. Mechanisms of Apnea. Progress in Cardiovascular Diseases, Vol. 51, No. 4 (January/February). pp. 313-323.

El, A.S., El, H., Palomo, J.M. & Baur, D.A. 2011. A 3-Dimensional Airway Analysis of an Obstructive Sleep Apnea Surgical Correction With Cone Beam Computed Tomography. American Association of Oral and Maxillofacial Surgeons. J Oral Maxillofac Surg 69. pp. 2424-2436.

Farré, R., Montserrat, J.M. & Navajas, D. 2008. Assessment of Upper Airway Mechanics During Sleep. Respiratory Physiology and Neurobiology 163. pp. 74-81

Flemons, W.W. & McNicholas, W.T. 1997. Clinical Prediction of the Sleep Apnea Syndrome. Sleep Medicine Reviews, Vol. 1, No. 1. pp. 19-32.

Huang, R.H., Li, X.P. & Rong, Q.G. 2013. Control Mechanism For the Upper Airway Collapse in Patients with Obstructive Sleep Apnea Syndrome: A Finite Element Study. Science China, Life Sciences Vol. 56. pp. 366-372.

Huang, Y., Malhorta, A. & White, D.P. 2003. A Computational Model of Upper Airway Colllapsibility. Proceedings of the 25th Annual International Conference of the IEEE EMBS Cancun, Mexico, September 17-21, 2003. p. 370.

Huang, Y., Malhorta, A. & White, D.P. 2005. Computational Simulation of Human Upper Airway Collapse Using a Pressure-/State-Dependent Model of Genioglossal Muscle Contraction Under Laminar Flow Conditions. Journal of Applied Physiology. pp. 1138-1148.

Huang, Y., White, D.P. & Malhorta, A. 2007. Use of Computational Modeling to Predict Responses to Upper Airway Surgery in Obstructive Sleep Apnea. The Laryngoscope 117. pp. 648-653.

Huang, Y., White, D.P. & Malhotra, A. 2012. The Impact of Anatomic Manipulations on Pharyngeal Collapse: Results From a Computational Model of the Normal Human Upper Airway. Author manuscript. Available in PMC. 13p.

Ito, Y., Cheng, G.C., Shih, A.M., Koomullil, R.P., Soni, B.K., Sittitavornwong, S. & Waite, P.D. 2011. Patient-Specific Geometry Modeling and Mesh Generation for

Simulating Obstructive Sleep Apnea Syndrome Cases by Maxillomandibular Advancement. Mathematics and Computers in Simulation 81. pp. 1876-1891.

Iwasaki, T., Saito, I., Takemoto, Y., Inada, E., Kanomi, R., Hayasaki, H. & Yamasaki, Y. 2011. Evaluation of Upper Airway Obstruction in Class II Children with Fluid-Mechanical Simulation. American Journal of Orthodontics and Dentofacial Orthopedics. pp. 135-145.

Jeong, S.-J., Kim, W.-S. & Sung, S.-J. 2006. Numerical investigation on the flow characteristics and aerodynamic force of the upper airway of patient with obstructive sleep apnea using computational fluid dynamics. Medical Engineering & Physics 29. pp. 637-651.

Jordan, A.S. & White, D.P. 2008. Pharyngeal Motor Control and the Pathogenesis of Obstructive Sleep Apnea. Respiratory Physiology & Neurobiology. pp. 1-7.
Lam, C.M.J., Sharma, S.K. & Lam, B. 2010. Obstructive sleep apnoea: Definitions, epidemiology & natural history. Indian Journal of Medical Research vol. 131. pp. 165-170.

Lee, C.-C., Chen & C.-W. 2009. The Impact of Sleep Apnea on Conventional Doppler Indices. Tzu Chi Medical Journal vol. 21, no. 3.

Liu, J., Udupa, J.K., Odhnera, D., McDonough, J.M., Raanan Arens, R. 2003. System for Upper Airway Segmentation and Measurement with MR Imaging and Fuzzy Connectedness. Academic Radiology Vol. 10, No. 1. pp. 13-24.

Lucey, A.D., King, A.J.C., Tetlow, G.A., Wang, J., Armstrong, J.J., Leigh, M.S., Paduch, A., Walsh, J.H., Sampson, D.D., Eastwood, P.R. & Hillman, D.R. 2010. Measurement, Reconstruction, and Flow-Field Computation of the Human Pharynx With Application to Sleep Apnea. IEEE Transactions on Biomedical Engineering, vol. 57, No. 10. pp. 2535-2548.

Marieb, N.E. & Hoehn, K. Human Anatomy and Physiology, 7th edition. 2007. Pearson Education, Inc.

Mihaescu M., Murugappan S., Gutmark E, Donnelly L.F., Khosla S. & Kalra M. 2008. Computational Fluid Dynamics Analysis of Upper Airway Reconstructed from Magnetic Resonance Imaging Data. Ann Otol Rhinol Laryngol.

Mihaescu, M., Murugappan, S., Kalra, M., Khosla, S. & Gutmark, E. 2008. Large Eddy Simulation and Reynolds-Averaged Navier–Stokes Modeling of Flow in a Realistic

Pharyngeal Airway Model: An Investigation of Obstructive Sleep Apnea. Journal of Biomechanics 41. pp. 2279-2288.

Mihaescu, M., Myalavarapu, G., Gutmark, E.J. & Powell, N.B. 2011. Large Eddy Simulation of the pharyngeal Airflow Associated with Obstructive Sleep Apnea Syndrome at Pre- and Post-Surgical Treatment. Journal of Biomechanics 44. pp. 2221-2228.

Myalavarapu, G., Mihaescu, M., Fuchs, L., Papatziamos, G. & Gutmark, E. 2013. Planning Human Upper Airway Surgery Using Computational Fluid Dynamics. Journal of Biomechanics 46. pp. 1979-1986.

Mylavarapu, G., Shanmugam, M., Mihaescu, M., Kalra, M., Khosla, S. & Gutmark, E. 2009. Validation of Computational Fluid Dynamics Methodology Used for Human Upper Airway Simulations. Journal of Biomechanics 42. pp. 1553-1559.

Persak, S.C., Sin, S., McDonough, J.M., Arens, R. & Wootton, D.M. 2011 Noninvasive Estimation of Pharyngeal Airway Resistance and Compliance in Children Based on Volume-Gated Dynamic MRI and Computational Fluid Dynamics. Journal of Applied Physiology Vol. 111. pp.1819-1827.

Powell, N.B., Mihaescu, M., Mylavarapu, G., Weaver, E.M., Guilleminault, C. & Gutmark, E. 2011. Patterns in Pharyngeal Airflow Associated with Sleep-Disordered Breathing. Sleep Medicine 12. pp. 966-974.

Sarasaen, C., Bhongmakapat, T., Hemtiwakorn, K., Laothamatas, J. & Pintavirooj, C. 2012. Computational Fluid Dynamic (CFD) in Thai Patient with Obstructive Sleep Apnea Syndrome (OSAS). A Case Report: Comparative Study Between Healthy and OSA Subject. The 2012 Biomedical Engineering International Conference. 6p.

Shin, L.K., Holdbrook, A.B., Capasso, R., Kushida, C.A., Powell, N.B., Fischbein, N.J. & Pauly, K.B. 2013. Improved Sleep MRI at 3 Tesla in Patients With Obstructive Sleep Apnea Journal of Magnetic Resonance Imaging. 6p.

Simon, H. & Zieve, D. 2012. Obstructive sleep apnea. [WWW]. [Accessed on 29.07.2013]. Available at: http://umm.edu/health/medical/reports/articles/obstructive-sleep-apnea

Stupak, H.D. 2010. The Human External Nose and its Evolutionary Role in the Prevention of Obstructive Sleep Apnea. Otolaryngology-Head and Neck Surgery. pp. 779-782.

Sung, S.-J., Jeong, S.-J., Yu, Y.-S., Hwang, C.-J. & Pae, E.-K. 2006. Customized Three-dimensional Computational Fluid Dynamics Simulation of the Upper Airway of Obstructive Sleep Apnea. Angle Orthodontist, Vol. 76, No. 5. pp. 791-799.

Susarla, S.M., Thomas, R.J., Abramson, Z.R. & Kaban, L.B. 2010. Biomechanics of the Upper Airway: Changing Concepts in the Pathogenesis of Obstructive Sleep Apnea. International Association of Oral and Maxillofacial Surgeons 39. pp. 1149-1159.

Trzebski, A. & Smietanowski, M. 2001. Non-Linear Dynamics of Cardiovascular System in Humans Exposed to Repetitive Apneas Modeling Obstructive Sleep Apnea: Aggregated Time Series Data Analysis. Autonomic Neuroscience: Basic and Clinical 90. pp. 106-115.

Van Holsbeke, C., Vos, W., Van Hoorenbeeck, K., Boudewyns, A., Salgado, R., Verdonck, P.R., Ramet, J., De Backer, J., De Backer, W. & Verhulst, S.L. 2013. Functional Respiratory Imaging as a Tool to Assess Upper Airway Patency in Children with Obstructive Sleep Apnea. Sleep Medicine 14. pp. 433-439.

Vos, W., De Backer, J., Devolder, A., Vanderverken, O., Verhulst, S., Salgado, R., Germonpre, P., Partoens, B., Wuyts, F., Parizel, P. & De Backer, W. 2007. Correlation Between Severity of Sleep Apnea and Upper Airway Morphology Based on Advanced Anatomical and Functional Imaging. Journal of Biomechanics 40. pp. 2207-2213.

Wang, Y. & Elghobashi. 2013. On locating the obstruction in the upper airway via numerical simulation. Respiratory Physiology & Neurobiology 193. pp. 1-10.

Wang, Y., Liu, Y., Sun, X., Chen, Z. & Gao, F. 2009. Evaluation of the Upper Airway in Children with Obstructive Sleep Apnea Undergoing Adenoidectomy Using Computational Fluid Dynamics. IEEE, National Natural Science Foundation of China. 4p.

Xu, C., Brennick, M.J. & Wootton, D.M. 2005. Image-Based Three-Dimensional Finite Element Modeling Approach for Upper Airway Mechanics. Proceeding of the 2005 IEEE Engineering in Medicine and Biology 27th Annual Conference Shanghai, China, September 1-4, 2005. pp. 2587-2590.

Xu, C., Brennick, M.J., Dougherty, L. & Wootton, D.M. 2009. Modeling Upper Airway Collapse by a Finite Element Model with Regional Tissue Properties. Medical Engineering & Physics 31. pp. 1343-1348.

Xu, C., Sin, S.H., McDonough, J.M., Udupa, J.K., Guez, A., Arens, R. & Wooton, D.M. 2006. Computational fluid dynamics modeling of the upper airway of children with obstructive sleep apnea syndrome in steady flow. Journal of Biomechanics 39. pp. 2043-2054.

Yu, C., Wang, G., Liu, Y. & Sun, X. 2009. 3D FE Model Reconstruction and Numerical Simulation of Airflow in Human Upper Airway for the Healthy Person and Patient with OSAS. IEEE, National Natural Science Foundation of China. 4p.

Yushkevich, A.P., Piven, J., Hazlett, H.C., Smith, R.G., Ho, S., Gee, J.C., & Guido, G. 2006. User-guided 3D active contour segmentation of anatomical structures: Significantly improved efficiency and reliability. Neuroimage, vol. 31 No. 3. pp. 1116-1128.

Zhao, M., Barber, T., Cistulli, P., Sutherland, K. & Rosengarten, G. 2013. Computational fluid dynamics for the assessment of upper airway response to oral appliance treatment in obstructive sleep apnea. Journal of Biomechanics 46. pp. 142-150.

Zhu, J.H., Lee, P.H., Lim, K.M., Lee, S.J., Teo, L.S.T. & Wang, D.Y. 2012. Passive movement of human soft palate during respiration: A simulation of 3D fluid/structure interaction. Journal of Biomechanics 45. pp. 1992-2000.

Appendix 1. Volumes of segmented structures

Table 1. *Volumes of segmented structures of patient 1*

Name of structure	**Pre-operative volume, cm^3**	**Post-operative volume, cm^3**	**Difference, cm^3**
Upper airway	18,17	17,25	-0,92
Lingual tonsils	6,82	7,80	0,98
Mylohyoid and hyloglossus muscles	15,00	15,30	0,30
Inner/outer masseter muscle	48,71	47,45	-1,26
Genioglossus muscle	55,77	59,41	3,64
Soft palate	4,82	3,15	-1,67
Stylo-pharyngeus muscle	15,62	16,68	1,06

Table 2. *Volumes of segmented structures of patient 2*

Name of structure	**Pre-operative volume, cm^3**	**Post-operative volume, cm^3**	**Difference, cm^3**
Upper airway	17,27	19,70	2,43
Lingual tonsils	5,88	6,72	0,84
Mylohyoid and hyloglossus muscles	25,10	27,37	2,27
Inner/outer masseter muscle	77,24	82,10	4,86
Genioglossus muscle	78,60	74,64	-3,96
Soft palate	8,56	7,75	-0,81
Stylo-pharyngeus muscle	16,20	12,70	-3,50

Table 3. *Volumes of segmented structures of patient 3*

Name of structure	**Pre-operative volume, cm^3**	**Post-operative volume, cm^3**	**Difference, cm^3**
Upper airway	15,08	16,68	1,60
Lingual tonsils	5,27	5,91	0,64
Mylohyoid and hyloglossus muscles	25,08	21,61	-3,47
Inner/outer masseter muscle	64,93	59,52	-5,41
Genioglossus muscle	61,01	51,17	-9,84
Soft palate	2,56	4,72	2,16
Stylo-pharyngeus muscle	11,89	12,23	0,34